

# Optimization and learning of quantum programs

Leonardo Banchi,<sup>1,2</sup> Jason Pereira,<sup>3</sup> Seth Lloyd,<sup>4,5</sup> and Stefano Pirandola<sup>3,5</sup>

<sup>1</sup>*Department of Physics and Astronomy, University of Florence,  
via G. Sansone 1, I-50019 Sesto Fiorentino (FI), Italy*

<sup>2</sup>*INFN Sezione di Firenze, via G.Sansone 1, I-50019 Sesto Fiorentino (FI), Italy*

<sup>3</sup>*Department of Computer Science, University of York, York YO10 5GH, UK*

<sup>4</sup>*Department of Mechanical Engineering, Massachusetts Institute of Technology (MIT), Cambridge MA 02139, USA*

<sup>5</sup>*Research Laboratory of Electronics, Massachusetts Institute of Technology (MIT), Cambridge MA 02139, USA*

A programmable quantum processor is a fundamental model of quantum computation. In this model, any quantum channel can be approximated by applying a fixed universal quantum operation onto an input state and a quantum “program” state, whose role is to condition the operation performed by the processor. It is known that perfect channel simulation is only possible in the limit of infinitely large program states, so that finding the best program state represents an open problem in the presence of realistic finite-dimensional resources. Here we prove that the search for the optimal quantum program is a convex optimization problem. This can be solved either exactly, by minimizing a diamond distance cost function via semi-definite programming, or approximately, by minimizing other cost functions via gradient-based machine learning methods. We apply this general result to a number of different designs for the programmable quantum processor, from the shallow protocol of quantum teleportation, to deeper schemes relying on port-based teleportation and parametric quantum circuits. We benchmark the various designs by investigating their optimal performance in simulating arbitrary unitaries, Pauli and amplitude damping channels.

## I. INTRODUCTION

Today the field of quantum computing [1] is becoming more and more mature, also thanks to the combined efforts of academic and industrial researchers. From a theoretical point of view, this endeavour is supported by increasing interconnections with other rapidly-advancing fields, such as machine learning [2]. For instance, we have recently witnessed the development of new hybrid areas of investigation, such as quantum-enhanced machine learning [3–7] (e.g., quantum neural networks, quantum annealing etc.), protocols of quantum-inspired machine learning (e.g., for recommendation systems [8] or component analysis and supervised clustering [9]) and classical learning methods applied to quantum computers, as explored here in this manuscript.

In quantum computing, a fundamental model is the programmable quantum gate array or programmable quantum processor [10]. This is a quantum processor where a fixed quantum operation is applied to an input state and a program state. The role of the program state is to condition the quantum operation in such a way to apply some target quantum gate or channel to the input state. This is a very flexible scheme but not actually universal: an arbitrary quantum channel cannot be programmed exactly, unless the program state is allowed to have an infinite number of qubits. For instance, a possible design relies on port-based teleportation (PBT) [11–13], where an input state is subject to certain local operations and classical communication (LOCCs) that are programmed by a tensor product of  $N$  bipartite states. For infinite  $N$ , any quantum channel can be simulated by copies of its Choi matrix [14] but, for any finite  $N$ , this simulation is not perfect.

Despite this fundamental model of quantum computa-

tion is known since 1997, a quantitative characterization of its actual performance in terms of gate implementation or channel simulation is still missing. Given a target quantum gate or channel, it is not yet known what degree of approximation can be reached and what kind of optimization procedure must be employed to choose the program state. After more than 20 years, the solution to these open problems comes from a suitable application of techniques of semidefinite programming (SDP) and machine learning (ML).

In our work, we quantify the error between an arbitrary target channel and its programmable simulation in terms of the diamond distance and other suitable cost functions, including the trace distance and the quantum fidelity. For all the considered cost functions, we are able to show that the minimization of the simulation error is a convex optimization problem in the space of the program states. This already solves an outstanding problem which affects various models of quantum computers (e.g., variational quantum circuits) where the optimization over classical parameters is non-convex and therefore not guaranteed to converge to a global optimum. By contrast, because our problem is proven to be convex, we can use SDP to minimize the diamond distance and always find the optimal program state for the simulation of a target channel, therefore optimizing the programmable quantum processor. Similarly, we may find suboptimal solutions by minimizing the trace distance or the quantum fidelity by means of gradient-based ML techniques, such as the projected subgradient method [15] and the conjugate gradient method [16, 17]. We note indeed that the minimization of the  $\ell_1$ -norm, mathematically related to the quantum trace distance, is widely employed in many ML tasks [18, 19], so many of those techniques can be adapted for learning program states.

With these general results in our hands, we first discuss the optimal learning of arbitrary unitaries with a generic programmable quantum processor. Then, we consider specific designs of the processor, from a shallow scheme based on the teleportation protocol, to higher-depth designs based on PBT [11–13] and parametric quantum circuits (PQCs) [20], introducing a suitable convex reformulation of the latter. In the various cases, we benchmark the processors for the simulation of basic unitary gates (qubit rotations) and various basic channels, including the amplitude damping channel which is known to be the most difficult to simulate [21, 22]. For the deeper designs, we find that the optimal program states do not correspond to the Choi matrices of the target channels, which is rather counter-intuitive and unexpected.

The paper is structured as follows. In Sec. II we discuss the general notion of programmable channel simulation, the various cost functions and a suitable Choi-reduction of the problem. In Sec. III we then show that the optimization of a generic programmable quantum processor is convex in the space of the program states. In Sec. IV we consider the optimization of the diamond distance via SDP and the minimization of the other cost functions via gradient descent. In particular, in Sec. V we provide the details of the gradient-based ML algorithms to be used, together with a discussion of smoothing techniques. In Sec. VI, we discuss the optimal learning of arbitrary unitaries. We then move to discuss the various specific designs based on teleportation (Sec. VII), PBT (Sec. VIII) and PQC (Sec. IX). Sec. X is for conclusions.

## II. PROGRAMMABLE SIMULATION

### A. General problem

Consider an arbitrary but known quantum channel  $\mathcal{E}$  from dimension  $d$  to dimension  $d'$  [1, 23]. We want to simulate  $\mathcal{E}$  using a programmable quantum processor [10] that we simply call “quantum processor” (see Fig. 1). This is represented by a completely positive trace-preserving (CPTP) universal map  $Q$  which is assumed to be fixed and applied to the arbitrary input  $\rho$  of the channel together with a program state  $\pi$  (which may be varied). In this way, the quantum processor generates an approximate channel  $\mathcal{E}_\pi$  as

$$\mathcal{E}_\pi(\rho) = \text{Tr}_2 [Q(\rho \otimes \pi)]. \quad (1)$$

Our goal is to find the program state  $\pi$  for which the simulation  $\mathcal{E}_\pi$  is the closest to  $\mathcal{E}$ , i.e., so that we minimize the following cost function

$$C_\diamond(\pi) := \|\mathcal{E} - \mathcal{E}_\pi\|_\diamond \leq 2, \quad (2)$$

in terms of the diamond distance [24, 25]. In other words,

$$\text{Find } \tilde{\pi} \text{ such that } C_\diamond(\tilde{\pi}) = \min_\pi C_\diamond(\pi). \quad (3)$$

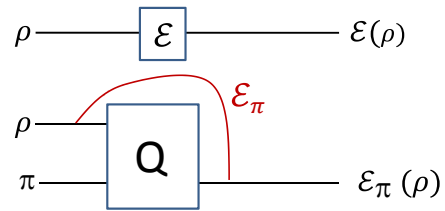


FIG. 1. Arbitrary quantum channel  $\mathcal{E}$  and its simulation  $\mathcal{E}_\pi$  via a quantum processor  $Q$  applied to a program state  $\pi$ .

From theory [10, 26] we know that we cannot achieve  $C_\diamond = 0$  for arbitrary  $\mathcal{E}$  unless  $\pi$  and  $Q$  have infinite dimensions. As a result, for any finite-dimensional realistic design of the quantum processor, finding the optimal program state  $\tilde{\pi}$  is an open problem.

Recall that the diamond distance is defined by the following maximization

$$\|\mathcal{E} - \mathcal{E}_\pi\|_\diamond = \max_\varphi \|\mathcal{I} \otimes \mathcal{E}(\varphi) - \mathcal{I} \otimes \mathcal{E}_\pi(\varphi)\|_1, \quad (4)$$

where  $\|O\|_1 := \text{Tr}\sqrt{O^\dagger O}$  is the trace norm [23]. Because the trace norm is convex over mixed states, one may reduce the maximization in Eq. (4) to bipartite pure states  $\varphi = |\varphi\rangle\langle\varphi|$ . In general, we therefore need to consider a min-max optimization, i.e., find  $\tilde{\pi}$  and (pure)  $\tilde{\varphi}$  such that

$$\begin{aligned} & \|\mathcal{I} \otimes \mathcal{E}(\tilde{\varphi}) - \mathcal{I} \otimes \mathcal{E}_\pi(\tilde{\varphi})\|_1 \\ & = \min_\pi \max_\varphi \|\mathcal{I} \otimes \mathcal{E}(\varphi) - \mathcal{I} \otimes \mathcal{E}_\pi(\varphi)\|_1. \end{aligned} \quad (5)$$

Also recall that the diamond distance can be computed using SDP [27]. In particular, due to strong duality, it may be computed via a minimization rather than a maximization, so that the min-max optimization problem in Eq. (5) can be transformed into a more convenient minimization problem (more details in Sec. IV A). An alternative solution is to reduce the general problem into a weaker one which is expressed in terms of the Choi matrix of the channel (see following section). In this way, we also avoid the maximization in  $\varphi$  but with the downside of using a larger cost function, the trace distance.

### B. Processor map and Choi reduction

It is known that a quantum channel  $\mathcal{E}$  is one-to-one with its Choi matrix  $\chi_\mathcal{E} := \mathcal{I} \otimes \mathcal{E}(\Phi)$ , where  $\Phi := |\Phi\rangle\langle\Phi|$  is  $d$ -dimensional maximally-entangled state, i.e.,

$$|\Phi\rangle := d^{-1/2} \sum_i |i, i\rangle. \quad (6)$$

Using the channel definition of Eq. (1), we may write

$$\begin{aligned} \chi_{\mathcal{E}_\pi} &= \mathcal{I} \otimes \mathcal{E}_\pi(\Phi) \\ &= d^{-1} \sum_{ij} |i\rangle\langle j| \otimes \text{Tr}_2 [Q(|i\rangle\langle j| \otimes \pi)]. \end{aligned} \quad (7)$$

From this expression, it is clear that the Choi matrix  $\chi_{\mathcal{E}}$  is linear in the program state  $\pi$ . More precisely, the Choi matrix  $\chi_{\mathcal{E}}$  at the output of the processor  $Q$  can be directly written as a CPTP linear map  $\Lambda$  acting on the space of the program states  $\pi$ , i.e.,

$$\chi_{\pi} := \chi_{\mathcal{E}\pi} = \Lambda(\pi). \quad (8)$$

This map is also depicted in Fig. 2.

We may connect the minimization of the diamond distance  $C_{\diamond}(\pi)$  to the minimization of the trace distance

$$C_1(\pi) := \|\chi_{\mathcal{E}} - \chi_{\pi}\|_1, \quad (9)$$

between the Choi matrices  $\chi_{\mathcal{E}}$  and  $\chi_{\pi}$ . In fact, we may write the sandwich relation [23]

$$C_1(\pi) \leq C_{\diamond}(\pi) \leq d C_1(\pi). \quad (10)$$

While the lower bound is immediate from the definition of Eq. (4), the upper bound can be proven using the following equivalent form of the diamond distance

$$\|\mathcal{E} - \mathcal{E}_{\pi}\|_{\diamond} = \sup_{\rho_0, \rho_1} d\|(\sqrt{\rho_0} \otimes \mathbb{1})(\chi_{\mathcal{E}} - \chi_{\pi})(\sqrt{\rho_1} \otimes \mathbb{1})\|_1, \quad (11)$$

where the optimization is done over the density matrices  $\rho_0$  and  $\rho_1$  [27, Theorem 3.1]. In fact, consider the Frobenius norm  $\|A\|_2 := \sqrt{\text{Tr}[A^{\dagger}A]}$  and the spectral norm

$$\|A\|_{\infty} := \max\{\|Au\| : u \in \mathbb{C}^d, \|u\| \leq 1\}, \quad (12)$$

which satisfy the following properties [23]

$$\|ABC\|_1 \leq \|A\|_{\infty} \|B\|_1 \|C\|_{\infty}, \quad (13)$$

$$\|A \otimes \mathbb{1}\|_{\infty} = \|A\|_{\infty} \leq \|A\|_2. \quad (14)$$

Then, from Eqs. (11), (13) and (14), one gets

$$\begin{aligned} \|\mathcal{E} - \mathcal{E}_{\pi}\|_{\diamond} &\leq \sup_{\rho_0, \rho_1} d\sqrt{\text{Tr}\rho_0 \text{Tr}\rho_1} \|\chi_{\mathcal{E}} - \chi_{\pi}\|_1 \\ &= d\|\chi_{\mathcal{E}} - \chi_{\pi}\|_1. \end{aligned} \quad (15)$$

Thanks to Eq. (10), we may avoid the maximization step in the definition of the diamond distance and simplify the original problem to approximating the Choi matrix  $\chi_{\mathcal{E}}$  of the channel by varying the program state  $\pi$ . This is a process of learning Choi matrices as depicted in Fig. 2. Because the simpler cost function  $C_1(\pi)$  is an upper bound, its minimization generally provides a sub-optimal solution for the program state.

### C. Other cost functions

Besides  $C_{\diamond}$  and  $C_1$  we can introduce other cost functions. First of all, using the Fuchs-van de Graaf inequality [28], we may write

$$C_1(\pi) \leq 2\sqrt{C_F(\pi)}, \quad C_F(\pi) = 1 - F(\pi)^2, \quad (16)$$

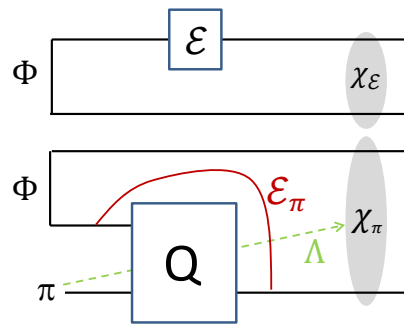


FIG. 2. Map of the processor and learning of Choi matrices. Consider an arbitrary (but known) quantum channel  $\mathcal{E}$  and its associated Choi matrix  $\chi_{\mathcal{E}}$ , generated by propagating part of a maximally-entangled state  $\Phi$ . Then, consider a quantum processor  $Q$  with program state  $\pi$  which generates the simulated channel  $\mathcal{E}_{\pi}$  and, therefore, the corresponding Choi matrix  $\chi_{\pi} := \chi_{\mathcal{E}\pi}$  upon propagating part of  $\Phi$  as input state. The map of the processor is the CPTP map  $\Lambda$  from the program state  $\pi$  to the output Choi matrix  $\chi_{\pi}$ . In a simplified version of our problem, we may optimize the program  $\pi$  in such a way to minimize the trace distance  $C_1(\pi) := \|\chi_{\mathcal{E}} - \chi_{\pi}\|_1$ .

where  $F(\pi)$  is Bures' fidelity between the two Choi matrices  $\chi_{\mathcal{E}}$  and  $\chi_{\pi}$ , i.e.,

$$F(\pi) := \|\sqrt{\chi_{\mathcal{E}}}\sqrt{\chi_{\pi}}\|_1 = \text{Tr}\sqrt{\chi_{\mathcal{E}}\chi_{\pi}\chi_{\mathcal{E}}}. \quad (17)$$

Another possible upper bound can be written using the quantum Pinsker's inequality [29, 30]. In fact, we may write  $C_1(\pi) \leq (2\ln\sqrt{2})\sqrt{C_R(\pi)}$ , where

$$C_R(\pi) := \min\{S(\chi_{\mathcal{E}}\|\chi_{\pi}), S(\chi_{\pi}\|\chi_{\mathcal{E}})\}, \quad (18)$$

and  $S(\rho\|\sigma) := \text{Tr}[\rho(\log_2\rho - \log_2\sigma)]$  is the quantum relative entropy between  $\rho$  and  $\sigma$ .

Finally we may consider other cost functions in terms of any Schatten  $p$ -norm  $C_p(\pi) := \|\chi_{\mathcal{E}} - \chi_{\pi}\|_p$ , even though this option provides lower bounds instead of upper bounds for the trace distance. Recall that, given an operator  $O$  and a real number  $p \geq 1$ , we may define its Schatten  $p$ -norm as [23]

$$\|O\|_p = (\text{Tr}|O|^p)^{1/p}, \quad (19)$$

where  $|O| = \sqrt{O^{\dagger}O}$ . For any  $1 \leq p \leq q \leq \infty$ , one has the monotony  $\|O\|_p \geq \|O\|_q$ , so that  $\|O\|_{\infty} \leq \dots \leq \|O\|_1$ . An important property is duality. For each pair of operators  $A$  and  $B$ , and each pair of parameters  $p, q \in [1, \infty]$  such that  $p^{-1} + q^{-1} = 1$ , we may write [23]

$$\|A\|_p = \sup_{\|B\|_q \leq 1} |\langle B, A \rangle| \equiv \sup_{\|B\|_q \leq 1} \langle B, A \rangle, \quad (20)$$

where  $\langle B, A \rangle = \text{Tr}(B^{\dagger}A)$  is the Hilbert-Schmidt product, and the second inequality follows since we can arbitrarily change the sign of  $B$ .

### III. CONVEXITY

In this section, we show that the minimization of the main cost functions  $C_\diamond$ ,  $C_1$  and  $C_F$  is a convex optimization problem in the space of the program states  $\pi$ . This means that we can find the optimal program state  $\tilde{\pi}$  by minimizing  $C_\diamond$  or, alternatively, sub-optimal program states can be found by minimizing either  $C_1$  or  $C_F$ . For the sake of generality we prove the result for all the cost functions discussed in the previous section.

**Theorem 1** *The minimization of the generic cost function  $C = C_\diamond, C_1, C_F, C_R$  or  $C_p$  for any  $p > 1$  is a convex optimization problem in the space of program states. In particular, the global minimum  $\tilde{\pi}$  can always be found as a local minimum of  $C_\diamond$ . Alternatively, this optimal program state can be approximated by minimizing  $C_1$  or  $C_F$ .*

*Proof.* Let us start to show the result for the diamond distance  $C_\diamond$ . In this case, we can write the following

$$\begin{aligned}
& C_\diamond[p\pi + (1-p)\pi'] \\
& := \|\mathcal{E} - \mathcal{E}_{p\pi+(1-p)\pi'}\|_\diamond \\
& \stackrel{(1)}{=} \|(p+1-p)\mathcal{E} - p\mathcal{E}_\pi - (1-p)\mathcal{E}_{\pi'}\|_\diamond \\
& \stackrel{(2)}{\leq} \|p\mathcal{E} - p\mathcal{E}_\pi\|_\diamond + \|(1-p)\mathcal{E} - (1-p)\mathcal{E}_{\pi'}\|_\diamond \\
& \stackrel{(3)}{\leq} p\|\mathcal{E} - \mathcal{E}_\pi\|_\diamond + (1-p)\|\mathcal{E} - \mathcal{E}_{\pi'}\|_\diamond \\
& = pC_\diamond(\pi) + (1-p)C_\diamond(\pi'), \tag{21}
\end{aligned}$$

where we use (1) the linearity of  $\mathcal{E}$ , (2) the triangle inequality and (3) the property  $\|xA\|_1 = |x|\|A\|_1$ , valid for any operator  $A$  and coefficient  $x$ .

For any Schatten  $p$ -norm  $C_p$  with  $p \geq 1$ , we may exploit the dual representation in Eq. (20) with  $A = \chi_\mathcal{E} - \Lambda(\pi)$ , so that

$$C_p(\pi) = \sup_{\|B\|_q \leq 1} |\text{Tr}\{B^\dagger[\chi_\mathcal{E} - \Lambda(\pi)]\}|. \tag{22}$$

For any convex combination  $\bar{\pi} := p_0\pi_0 + p_1\pi_1$ , with  $p_0 + p_1 = 1$ , we have  $\Lambda(\bar{\pi}) = p_0\Lambda(\pi_0) + p_1\Lambda(\pi_1)$  by linearity,

and we may write

$$\begin{aligned}
& C_p(\bar{\pi}) \\
& = \sup_{\|B\|_q \leq 1} |\text{Tr}\{B^\dagger[p_0\chi_\mathcal{E} + p_1\chi_\mathcal{E} - p_0\Lambda(\pi_0) - p_1\Lambda(\pi_1)]\}| \\
& \stackrel{(1)}{=} \sup_{\|B\|_q \leq 1} |\text{Tr}\{p_0B^\dagger[\chi_\mathcal{E} - \Lambda(\pi_0)] + p_1B^\dagger[\chi_\mathcal{E} - \Lambda(\pi_1)]\}| \\
& \stackrel{(2)}{=} \sup_{\|B\|_q \leq 1} |p_0\text{Tr}\{B^\dagger[\chi_\mathcal{E} - \Lambda(\pi_0)]\} + \\
& \quad + p_1\text{Tr}\{B^\dagger[\chi_\mathcal{E} - \Lambda(\pi_1)]\}| \\
& \stackrel{(3)}{\leq} \sup_{\|B\|_q \leq 1} |p_0\text{Tr}\{B^\dagger[\chi_\mathcal{E} - \Lambda(\pi_0)]\}| + \\
& \quad + |p_1\text{Tr}\{B^\dagger[\chi_\mathcal{E} - \Lambda(\pi_1)]\}| \\
& \stackrel{(4)}{\leq} p_0 \sup_{\|B\|_q \leq 1} |\text{Tr}\{B^\dagger[\chi_\mathcal{E} - \Lambda(\pi_0)]\}| + \\
& \quad + p_1 \sup_{\|C\|_q \leq 1} \text{Tr}\{C^\dagger[\chi_\mathcal{E} - \Lambda(\pi_1)]\} \\
& = p_0C(\pi_0) + p_1C(\pi_1), \tag{23}
\end{aligned}$$

where we use: (1) linearity of the operator  $B$ , (2) linearity of the trace, (3) triangle inequality, (4) and the inequality  $\sup_B f(B) + g(B) \leq \sup_B f(B) + \sup_C g(C)$  for the optimization of two functions.

To show the convexity of  $C_F$ , defined in Eq. (16), we note that the fidelity function  $F(\rho, \sigma)$  satisfies the following concavity relation [31]

$$F\left(\sum_k p_k \rho_k, \sigma\right)^2 \geq \sum_k p_k F(\rho_k, \sigma)^2. \tag{24}$$

Due to the linearity of  $\chi_\pi = \Lambda(\pi)$ , the fidelity in Eq. (17) satisfies  $F_{\bar{\pi}}^2 \geq \sum_k p_k F_{\pi_k}^2$  for  $\bar{\pi} := \sum_k p_k \pi_k$ . Accordingly, we get the following convexity result

$$C_F\left(\sum_k p_k \pi_k\right) \leq \sum_k p_k C_F(\pi_k). \tag{25}$$

For the cost function  $C_R$ , the result comes from the linearity of  $\Lambda(\pi)$  and the joint convexity of the relative entropy. In fact, for  $\bar{\pi} := p_0\pi_0 + p_1\pi_1$ , we may write

$$\begin{aligned}
S[\Lambda(\bar{\pi})|\chi_\mathcal{E}] & = S[p_0\Lambda(\pi_0) + p_1\Lambda(\pi_1)|\chi_\mathcal{E}] \\
& = S[p_0\Lambda(\pi_0) + p_1\Lambda(\pi_1)|p_0\chi_\mathcal{E} + p_1\chi_\mathcal{E}] \\
& \leq p_0S[\Lambda(\pi_0), \chi_\mathcal{E}] + p_1S[\Lambda(\pi_1), \chi_\mathcal{E}], \tag{26}
\end{aligned}$$

with symmetric proof for  $S[\chi_\mathcal{E}|\Lambda(\bar{\pi})]$ . This implies the convexity of  $C_R(\pi)$  in Eq. (18). ■

#### A. Convex classical parametrizations

The result of the theorem can certainly be extended to any convex parametrization of program states. For

instance, assume that  $\pi = \pi(\boldsymbol{\lambda})$ , where  $\boldsymbol{\lambda} = \{\lambda_i\}$  is a probability distribution. This means that, for  $0 \leq p \leq 1$  and any two parametrizations,  $\boldsymbol{\lambda}$  and  $\boldsymbol{\lambda}'$ , we may write

$$\pi[p\boldsymbol{\lambda} + (1-p)\boldsymbol{\lambda}'] = p\pi(\boldsymbol{\lambda}) + (1-p)\pi(\boldsymbol{\lambda}'). \quad (27)$$

Then the problem remains convex in  $\boldsymbol{\lambda}$  and we may therefore find the global minimum in these parameters. It is clear that this global minimum  $\tilde{\boldsymbol{\lambda}}$  identifies a program state  $\pi(\tilde{\boldsymbol{\lambda}})$  which is not generally the optimal state  $\tilde{\pi}$  in the entire program space  $\mathcal{S}$ , even though the solution may be a convenient solution for experimental applications.

Note that a possible classical parametrization consists of using classical program states, of the form

$$\pi(\boldsymbol{\lambda}) = \sum_i \lambda_i |\varphi_i\rangle \langle \varphi_i|, \quad (28)$$

where  $\{|\varphi_i\rangle\}$  is an orthonormal basis in the program space. Convex combinations of probability distributions therefore define a convex set of classical program states

$$\mathcal{S}_{\text{class}} = \{\pi : \pi = \sum_i \lambda_i |\varphi_i\rangle \langle \varphi_i|, \langle \varphi_i | \varphi_j \rangle = \delta_{ij}\}. \quad (29)$$

Optimizing over this specific subspace corresponds to optimizing the programmable quantum processor over classical programs. It is clear that global minima in  $\mathcal{S}_{\text{class}}$  and  $\mathcal{S}$  are expected to be very different. For instance,  $\mathcal{S}_{\text{class}}$  cannot certainly include Choi matrices which are usually very good quantum programs.

## IV. CONVEX OPTIMIZATION

### A. SDP minimization

Once we have Theorem 1 in our hands, we can successfully minimize the various cost functions in the search of the optimal program state. In other words, for a generic cost function  $C$  we want to solve  $\min_{\pi \in \mathcal{S}} C(\pi)$ . The solution is exact if we directly use the diamond-distance cost  $C_{\diamond}(\pi) = \|\mathcal{E} - \mathcal{E}_{\pi}\|_{\diamond}$  and we minimize it via SDP.

Let us introduce the linear map  $\Omega_{\pi} := \mathcal{E} - \mathcal{E}_{\pi}$  with corresponding Choi matrix

$$\chi_{\Omega_{\pi}} = \chi_{\mathcal{E}} - \chi_{\pi} = \chi_{\mathcal{E}} - \Lambda(\pi). \quad (30)$$

Thanks to the property of strong duality of the diamond norm, for any program  $\pi$  we can compute the cost function  $C_{\diamond}(\pi) = \|\Omega_{\pi}\|_{\diamond}$  via the following SDP [32]

$$\begin{aligned} & \text{Minimize } \frac{1}{2} (\|\text{Tr}_2 M_0\|_{\infty} + \|\text{Tr}_2 M_1\|_{\infty}), \\ & \text{Subject to } \begin{pmatrix} M_0 & -d \chi_{\Omega_{\pi}} \\ -d \chi_{\Omega_{\pi}}^{\dagger} & M_1 \end{pmatrix} \geq 0, \end{aligned} \quad (31)$$

where  $M_0 \geq 0$  and  $M_1 \geq 0$  in  $\mathbb{C}^{d \times d'}$ , and the spectral norm  $\|O\|_{\infty}$  equals the maximum singular value of  $O$ .

Moreover, because  $\chi_{\Omega_{\pi}}$  is Hermitian, the above SDP can be simplified into

$$\begin{aligned} & \text{Minimize } 2 \|\text{Tr}_2 Z\|_{\infty}, \\ & \text{Subject to } Z \geq 0 \text{ and } Z \geq d \chi_{\Omega_{\pi}}. \end{aligned} \quad (32)$$

Not only this procedure computes  $C_{\diamond}(\pi)$  but also provides the upper bound  $C_{\diamond}(\pi) \leq d \|\text{Tr}_2 |\chi_{\mathcal{E}} - \chi_{\pi}|\|_{\infty}$  [33]. In fact, it is sufficient to choose  $Z = d \chi_{\Omega_{\pi}}^+$ , where  $\chi^+ = (\chi + |\chi|)/2$  is the positive part of  $\chi$ . Using  $\text{Tr}_2 \chi_{\Omega_{\pi}} = 0$ , we may write  $\text{Tr}_2 Z \leq d \text{Tr}_2 \chi_{\Omega_{\pi}}^+ = \frac{d}{2} \text{Tr}_2 |\chi_{\Omega_{\pi}}|$ .

The SDP form in Eq. (32) is particularly convenient for finding the optimal program. In fact, suppose now that  $\pi$  is not fixed but we want to optimize on this state too, so as to compute the optimal program state  $\tilde{\pi}$  such that  $C_{\diamond}(\tilde{\pi}) = \min_{\pi \in \mathcal{S}} C_{\diamond}(\pi)$ . The problem is therefore mapped into the following unique minimization

$$\begin{aligned} & \text{Minimize } 2 \|\text{Tr}_2 Z\|_{\infty}, \\ & \text{Subject to } Z \geq 0, \pi \geq 0, \text{Tr}(\pi) = 1, Z \geq d \chi_{\Omega_{\pi}}. \end{aligned} \quad (33)$$

This algorithm can be used to optimize the performance of any programmable quantum processor.

### B. Gradient descent

An alternative approach (useful for deeper processors) consists in the optimization of the larger but easier-to-compute cost function  $C = C_1$  (trace distance) or  $C_F$  (infidelity). According to Theorem 1, the cost function  $C : \mathcal{S} \rightarrow \mathbb{R}$  is convex over the program space  $\mathcal{S}$  and, therefore, we can solve the optimization  $\min_{\pi \in \mathcal{S}} C(\pi)$  by using gradient-based ML algorithms. This means that we need to compute the derivatives of  $C$  and use gradient descent in order to converge to a local (global) minimum.

The sub-differential of  $C$  at the generic point  $\pi \in \mathcal{S}$  is defined as

$$\partial C(\pi) = \{Z : C(\sigma) - C(\pi) \geq \text{Tr}[Z(\sigma - \pi)], \forall \sigma \in \mathcal{S}\} \quad (34)$$

where  $Z$  is Hermitian [34, 35]. In the points where  $C$  is not only convex but also differentiable, then

$$\partial C(\pi) = \{\nabla C(\pi)\}, \quad (35)$$

namely the subgradient contains a single element, the gradient  $\nabla C$ , that can be obtained as the Fréchet derivative of  $C$  (for more details see Appendix A). In the points where  $C$  is not differentiable, then the gradient still provides an element of the subgradient to be used in the gradient-based minimization process.

In order to compute the gradient  $\nabla C$ , it is convenient to consider the Kraus decomposition of the processor map  $\Lambda$ . Let us write

$$\Lambda(\pi) = \sum_k A_k \pi A_k^{\dagger}, \quad (36)$$

with Kraus operators  $A_k$ . We then define the dual map  $\Lambda^*$  of the processor as the one (generally non-trace-preserving) which is given by the following decomposition

$$\Lambda^*(\rho) = \sum_k A_k^\dagger \rho A_k. \quad (37)$$

With these definitions in hands, we prove the following.

**Theorem 2** *Suppose we use a quantum processor  $Q$  with map  $\Lambda(\pi) = \chi_\pi$  in order to approximate the Choi matrix  $\chi_\mathcal{E}$  of an arbitrary channel  $\mathcal{E}$ . Then, the gradients of the trace distance  $C_1(\pi)$  and the infidelity  $C_F(\pi)$  are given by the following analytical formulas*

$$\nabla C_1(\pi) = \sum_k \text{sign}(\lambda_k) \Lambda^*(P_k), \quad (38)$$

$$\nabla C_F(\pi) = -2\sqrt{1 - C_F(\pi)} \nabla F(\pi), \quad (39)$$

$$\nabla F(\pi) = \frac{1}{2} \Lambda^* \left[ \sqrt{\chi_\mathcal{E}} (\sqrt{\chi_\mathcal{E}} \Lambda(\pi) \sqrt{\chi_\mathcal{E}})^{-\frac{1}{2}} \sqrt{\chi_\mathcal{E}} \right], \quad (40)$$

where  $\lambda_k$  ( $P_k$ ) are the eigenvalues (eigenprojectors) of the Hermitian operator  $\chi_\pi - \chi_\mathcal{E}$ . When  $C_1(\pi)$  or  $C_F(\pi)$  are not differentiable at  $\pi$ , then the above expressions provide an element of the subgradient  $\partial C(\pi)$ .

**Proof.** We prove the above theorem assuming that the functions are differentiable for program  $\pi$ . For non-differentiable points, the only difference is that the above analytical expressions are not unique and provide only one of the possibly infinite elements of the subgradient. Further details of this mathematical proof are given in Appendix A. Following matrix differentiation (see Appendix A 1), for any function  $f(A) = \text{Tr}[g(A)]$  of a matrix  $A$ , we may write

$$d\text{Tr}[g(A)] = \text{Tr}[g'(A)dA], \quad (41)$$

and the gradient is  $\nabla f(A) = g'(A)$ . Both the trace-distance and fidelity cost functions can be written in this form. To find the explicit gradient of the fidelity function we first note that, by linearity, we may write

$$\Lambda(\pi + \delta\pi) = \Lambda(\pi) + \Lambda(\delta\pi), \quad (42)$$

and therefore the following expansion

$$\begin{aligned} & \sqrt{\chi_\mathcal{E}} \Lambda(\pi + \delta\pi) \sqrt{\chi_\mathcal{E}} = \\ & \sqrt{\chi_\mathcal{E}} \Lambda(\pi) \sqrt{\chi_\mathcal{E}} + \sqrt{\chi_\mathcal{E}} \Lambda(\delta\pi) \sqrt{\chi_\mathcal{E}}. \end{aligned} \quad (43)$$

From this equation and differential calculations of the fidelity (see Appendix A 2 for details), we find

$$dF = \frac{1}{2} \text{Tr} \left[ (\sqrt{\chi_\mathcal{E}} \Lambda(\pi) \sqrt{\chi_\mathcal{E}})^{-\frac{1}{2}} \sqrt{\chi_\mathcal{E}} \Lambda(\delta\pi) \sqrt{\chi_\mathcal{E}} \right], \quad (44)$$

where  $dF = F(\pi + \delta\pi) - F(\pi)$ . Then, using the cyclic property of the trace, we get

$$dF = \frac{1}{2} \text{Tr} \left[ \Lambda^* \left[ \sqrt{\chi_\mathcal{E}} (\sqrt{\chi_\mathcal{E}} \Lambda(\pi) \sqrt{\chi_\mathcal{E}})^{-\frac{1}{2}} \sqrt{\chi_\mathcal{E}} \right] \delta\pi \right]. \quad (45)$$

Exploiting this expression in Eq. (41) we get the gradient  $\nabla F(\pi)$  as in Eq. (40). The other Eq. (39) simply follows from applying the definition in Eq. (16).

For the trace distance, let us write the eigenvalue decomposition

$$\chi_\pi - \chi_\mathcal{E} = \sum_k \lambda_k P_k. \quad (46)$$

Then using linearity of Eq. (42), the definition of processor map of Eq. (8) and differential calculations of the trace distance (see Appendix A 3 for details), we can write

$$\begin{aligned} dC_1(\pi) &= \sum_k \text{sign}(\lambda_k) \text{Tr}[P_k \Lambda(d\pi)] \\ &= \sum_k \text{sign}(\lambda_k) \text{Tr}[\Lambda^*(P_k) d\pi] \\ &= \text{Tr} \{ \Lambda^* [\text{sign}(\chi_\pi - \chi_\mathcal{E})] d\pi \}. \end{aligned} \quad (47)$$

From the definition of the gradient in Eq. (41), we finally get

$$\nabla C_1(\pi) = \Lambda^* [\text{sign}(\chi_\pi - \chi_\mathcal{E})], \quad (48)$$

which leads to the result in Eq. (38). ■

The above results in Eqs. (39) and (38) can be used together with the projected subgradient method [15] or conjugate gradient algorithm [16, 17] to iteratively find the optimal program state in the minimization of  $\min_{\pi \in \mathcal{S}} C(\pi)$  for  $C = C_1$  or  $C_F$ . In the following section we present the details of the two mentioned gradient-based ML algorithms and how they can be adapted for the learning of program states.

## V. GRADIENT-BASED CONVEX OPTIMIZATION TECHNIQUES

Gradient-based convex optimization is at the heart of many popular ML techniques such as, online learning in a high-dimensional feature space [18], missing value estimation problems [19], text classification, image ranking, and optical character recognition [36], to name a few. In all the above applications, “learning” corresponds to the following minimization problem  $\min_{x \in \mathcal{S}} f(x)$ , where  $f(x)$  is a convex function and  $\mathcal{S}$  is a convex set. Quantum learning falls into this category, as the space of program states is convex due to the linearity of quantum mechanics and cost functions are typically convex in this space (see Theorem 1). Gradient-based approaches are among the most applied methods for convex optimization of non-linear, possibly non-smooth functions [34]. Here we present two algorithms, the projected subgradient method and the conjugate gradient method, and show how that can be adapted to our problem.

Projected subgradient methods have the advantage of simplicity and the ability to optimize non-smooth functions, but can be slower, with a convergence rate  $\mathcal{O}(\epsilon^{-2})$

for a desired accuracy  $\epsilon$ . Conjugate gradient methods [16, 17] have a faster convergence rate  $\mathcal{O}(\epsilon^{-1})$ , provided that the cost function is smooth. This convergence rate can be improved even further to  $\mathcal{O}(\epsilon^{-1/2})$  for strongly convex functions [37] or using Nesterov's accelerated gradient method [38]. The technical difficulty in the adaptation of these methods for learning program states comes because the latter is a constrained optimization problem, namely at each iteration step the optimal program must be a proper quantum state, and the cost functions coming from quantum information theory are, generally, non-smooth.

### A. Projected subgradient method

Given the space  $\mathcal{S}$  of program states, let us define the projection  $\mathcal{P}_{\mathcal{S}}$  onto  $\mathcal{S}$  as

$$\mathcal{P}_{\mathcal{S}}(X) = \operatorname{argmin}_{\pi \in \mathcal{S}} \|X - \pi\|_2, \quad (49)$$

where  $\operatorname{argmin}$  is the argument of the minimum, namely the closest state  $\pi \in \mathcal{S}$  to the operator  $X$ . Then, a first order algorithm to solve  $\min_{\pi \in \mathcal{S}} C(\pi)$  is to apply the projected subgradient method [15, 34], which iteratively applies the following steps

- 1) Select an operator  $g_i$  from  $\partial C(\pi_i)$ ,
- 2) Update  $\pi_{i+1} = \mathcal{P}_{\mathcal{S}}(\pi_i - \alpha_i g_i)$ ,

where  $i$  is the iteration index and  $\alpha_i$  a learning rate.

The above algorithm differs from standard gradient methods in two aspects: i) the update rule is based on the subgradient, which is defined even for non-smooth functions; ii) the operator  $\pi_i - \alpha_i g_i$  is generally not a quantum state, so the algorithm fixes this issue by projecting that operator back to the closest quantum state, via Eq. (49). The algorithm converges to the optimal solution  $\pi_*$  (approximating the optimal program  $\tilde{\pi}$ ) as [15]

$$C(\pi_i) - C(\pi_*) \leq \frac{e_1 + G \sum_{k=1}^i \alpha_k^2}{2 \sum_{k=1}^i \alpha_k} =: \epsilon, \quad (51)$$

where  $e_1 = \|\pi_1 - \pi_*\|_2^2$  is the initial error (in Frobenius norm) and  $G$  is such that  $\|g\|_2^2 \leq G$  for any  $g \in \partial C$ . Popular choices for the learning rate that assure convergence are  $\alpha_k \propto 1/\sqrt{k}$  and  $\alpha_k = a/(b+k)$  for some  $a, b > 0$ .

In general, the projection step is the major drawback, which often limits the applicability of the projected subgradient method to practical problems. Indeed, projections like Eq. (49) require another full optimization at each iteration that might be computationally intensive. Nonetheless, we show in the following theorem that this issue does not occur in learning quantum states, because the resulting optimization can be solved analytically.

**Theorem 3** *Let  $X$  be a Hermitian operator in a  $d$ -dimensional Hilbert space with spectral decomposition*

*$X = UxU^\dagger$ , where the eigenvalues  $x_j$  are ordered in decreasing order. Then  $\mathcal{P}_{\mathcal{S}}(X)$  of Eq. (49) is given by*

$$\mathcal{P}_{\mathcal{S}}(X) = U\lambda U^\dagger, \quad \lambda_i = \max\{x_i - \theta, 0\}, \quad (52)$$

where  $\theta = \frac{1}{s} \sum_{j=1}^s (x_j - 1)$  and

$$s = \max \left\{ k \in [1, \dots, d] : x_k > \frac{1}{k} \sum_{j=1}^k (x_j - 1) \right\}. \quad (53)$$

**Proof.** Any quantum (program) state can be written in the diagonal form  $\pi = V\lambda V^\dagger$  where  $V$  is a unitary matrix, and  $\lambda$  is the vector of eigenvalues in decreasing order, with  $\lambda_j \geq 0$  and  $\sum_j \lambda_j = 1$ . To find the optimal state, it is required to find both the optimal unitary  $V$  and the optimal eigenvalues  $\lambda$  with the above property, i.e.,

$$\mathcal{P}_{\mathcal{S}}(X) = \operatorname{argmin}_{V, \lambda} \|X - V\lambda V^\dagger\|_2. \quad (54)$$

For any unitarily-invariant norm, the following inequality holds [39, Eq. IV.64]

$$\|X - \pi\|_2 \geq \|x - \lambda\|_2, \quad (55)$$

with equality when  $U = V$ , where  $X = UxU^\dagger$  is a spectral decomposition of  $X$  such that the  $x_j$ 's are in decreasing order. This shows that the optimal unitary in Eq. (54) is the diagonalization matrix of the operator  $X$ . The eigenvalues of any density operator form a probability simplex. The optimal eigenvalues  $\lambda$  are then obtained thanks to Algorithm 1 from Ref. [18]. ■

In the following section we present an alternative algorithm with faster convergence rates, but stronger requirements on the function to be optimized.

### B. Conjugate gradient method

The conjugate gradient method [16, 34], sometimes called Frank-Wolfe algorithm, has been developed to provide better convergence speed and to avoid the projection step at each iteration. Although the latter can be explicitly computed for quantum states (thanks to our Theorem 3), having a faster convergence rate is important, especially with higher dimensional Hilbert spaces. The downside of this method is that it necessarily requires a differentiable cost function  $C$ , with gradient  $\nabla C$ .

In its standard form, the conjugate gradient method to approximate the solution of  $\operatorname{argmin}_{\pi \in \mathcal{S}} C(\pi)$  is defined by the following iterative rule

- 1) Find  $\operatorname{argmin}_{\sigma \in \mathcal{S}} \operatorname{Tr}[\sigma \nabla C(\pi_i)]$ ,
- 2)  $\pi_{i+1} = \pi_i + \frac{2}{i+2}(\sigma - \pi_i) = \frac{i}{i+2}\pi_i + \frac{2}{i+2}\sigma$ .

The first step in the above iteration rule is solved by finding the smallest eigenvector  $|\sigma\rangle$  of  $\nabla C(\pi_i)$ . Indeed, since  $\pi$  is an operator and  $C(\pi)$  a scalar, the gradient  $\nabla C$  is

an operator with the same dimension of  $\pi$ . Therefore, for learning quantum programs we find the following iteration following

- 1) Find the smallest eigenvalue  $|\sigma_i\rangle$  of  $\nabla C(\pi_i)$ ,
  - 2)  $\pi_{i+1} = \frac{i}{i+2}\pi_i + \frac{2}{i+2}|\sigma_i\rangle\langle\sigma_i|$ .
- (57)

When the gradient of  $C$  is Lipschitz continuous with constant  $L$ , the conjugate gradient method converges after  $\mathcal{O}(L/\epsilon)$  steps [17, 38]. The following iteration with adaptive learning rate  $\alpha_i$  has even faster convergence rates, provided that  $C$  is strongly convex [37]:

- 1) Find the smallest eigenvalue  $|\sigma_i\rangle$  of  $\nabla C(\pi_i)$ ,
  - 2) Find  $\alpha_i = \operatorname{argmin}_{\alpha \in [0,1]} \alpha \langle \tau_i, \nabla C(\pi_i) \rangle + \alpha^2 \frac{\beta_C}{2} \|\tau_i\|_C^2$ , for  $\tau_i = |\sigma_i\rangle\langle\sigma_i| - \pi_i$ ,
  - 3)  $\pi_{i+1} = (1 - \alpha_i)\pi_i + \alpha_i |\sigma_i\rangle\langle\sigma_i|$ .
- (58)

where the constant  $\beta_C$  and norm  $\|\cdot\|_C$  depend on  $C$  [37].

In spite of the faster convergence rate, conjugate gradient methods require smooth cost functions (so that the gradient  $\nabla C$  is well defined at every point). However, cost functions based on trace distance (9) are not smooth. For instance, the trace distance in one-dimensional spaces reduces to the absolute value function  $|x|$  that is non-analytic at  $x = 0$ . When some eigenvalues are close to zero, conjugate gradient methods may display unexpected behaviors, though we have numerically observed that convergence is always obtained with a careful choice of the learning rate. Moreover, in the next section we will show how to formally justify the applicability of the conjugate gradient method, following Nesterov's smoothing prescription [38].

### C. Smooth trace distance

The conjugate gradient method converges to the global optimum after  $\mathcal{O}(\frac{L}{\epsilon})$  steps, provided that the gradient of  $C$  is  $L$ -Lipschitz continuous [38]. However, the constant  $L$  can diverge for non-smooth functions like the trace distance (9) so the convergence of the algorithm cannot be formally stated, although it may still be observed in numerical simulations, as we will show. To solidify the convergence proof (see also Appendix B 2) we introduce a smooth approximation to the trace distance. This is defined by the following cost function that is differentiable at every point

$$C_\mu(\pi) = \operatorname{Tr} [h_\mu(\chi_\pi - \chi_\mathcal{E})] = \sum_j h_\mu(\lambda_j), \quad (59)$$

where  $\lambda_j$  are the eigenvalues of  $\chi_\pi - \chi_\mathcal{E}$  and  $h_\mu$  is the so-called Huber penalty function

$$h_\mu(x) := \begin{cases} \frac{x^2}{2\mu} & \text{if } |x| < \mu, \\ |x| - \frac{\mu}{2} & \text{if } |x| \leq \mu. \end{cases} \quad (60)$$

The previous definition of the trace distance,  $C_1$  in Eq. (9), is recovered for  $\mu \rightarrow 0$  and, for any non-zero  $\mu$ , the  $C_\mu$  bounds  $C_1$  as follows

$$C_\mu(\pi) \leq C_1(\pi) \leq C_\mu(\pi) + \frac{\mu d}{2}, \quad (61)$$

where  $d$  is the dimension of the program state  $\pi$ . In Appendix B 2 we then prove the following result

**Theorem 4** *The smooth cost function  $C_\mu(\pi)$  is a convex function over program states and its gradient is given by*

$$\nabla C_\mu(\pi) = \Lambda^* [h'_\mu(\chi_\pi - \chi_\mathcal{E})], \quad (62)$$

where  $h'_\mu$  is the derivative of  $h_\mu$ . Moreover, the gradient is  $L$ -Lipschitz continuous with

$$L = \frac{d}{\mu}, \quad (63)$$

where  $d$  is the dimension of the program state.

Being Lipschitz continuous, the conjugate gradient algorithm and its variants [37, 38] converge up to an accuracy  $\epsilon$  after  $\mathcal{O}(L/\epsilon)$  steps. In some applications, it is desirable to analyze the convergence in trace distance in the limit of large program states, namely for  $d \rightarrow \infty$ . The parameter  $\mu$  can be chosen such that the smooth trace distance converges to the trace distance, namely  $C_\mu \rightarrow C_1$  for  $d \rightarrow \infty$ . Indeed, given the inequality (61), a possibility is to set  $\mu = \mathcal{O}(d^{-(1+\eta)})$  for some  $\eta > 0$  so that, from Eq. (63), the convergence to the trace norm is achieved after  $\mathcal{O}(d^{2+\eta})$  steps.

## VI. LEARNING OF ARBITRARY UNITARIES

The simulation of quantum gates or, more generally, unitary transformations is crucial for quantum computing applications [20] so ML techniques have been developed for this purpose [40–43]. Here we consider the more general setting of simulating an arbitrary finite-dimensional unitary  $U$  by means of a programmable quantum processor with map  $\Lambda$ . For a unitary  $U$  the Choi matrix is a maximally-entangled pure state  $\chi_\mathcal{E} = |\chi_U\rangle\langle\chi_U|$ . Therefore,  $\sqrt{\chi_\mathcal{E}} = \chi_\mathcal{E}$  is a one-dimensional projector and Eq. (40) is drastically simplified to

$$\nabla F(\pi) = \frac{\Lambda^* [|\chi_U\rangle\langle\chi_U|]}{2\sqrt{\langle\chi_U|\Lambda(\pi)|\chi_U\rangle}}. \quad (64)$$

Therefore the gradient (39) of the convex cost function  $C_F$ ,

$$\nabla C_F(\pi) = -\Lambda^* [|\chi_U\rangle\langle\chi_U|], \quad (65)$$

is independent of  $\pi$ . When we employ the conjugate gradient method, the state  $|\sigma_k\rangle$  is the same for each iteration step. This implies that conjugate gradient is converging

towards one eigenvector of  $-\Lambda^* [|\chi_U\rangle\langle\chi_U|]$  with minimum eigenvalue. In other terms, the fixed point of the iteration in Eq. (57), namely the optimal program state  $\tilde{\pi}_F$  (according to the fidelity cost function) is pure and equal to the eigenvector of  $\Lambda^* [|\chi_U\rangle\langle\chi_U|]$  with maximum eigenvalue.

The above result can be proven as follows. Let  $\pi_1$  be the initial guess for the program state. After  $k$  iterations of Eq. (57), we find the following approximation to the optimal program state

$$\pi_k = \frac{2}{k+k^2}\pi_1 + \left(1 - \frac{2}{k+k^2}\right)\tilde{\pi}_F, \quad (66)$$

where  $\frac{2}{k+k^2} = \prod_{j=1}^{k-1} \frac{j}{j+2}$ . The above equation shows that  $\pi_k \rightarrow \tilde{\pi}_F$  for  $k \rightarrow \infty$ , with error in trace distance

$$\|\pi_k - \tilde{\pi}_F\|_1 = \frac{2}{k+k^2} \|\pi_1 - \tilde{\pi}_F\|_1 = \mathcal{O}(k^{-2}). \quad (67)$$

For learning arbitrary unitaries, the fidelity cost function provides a convenient choice where the optimal program can be found analytically. Moreover, this example shows that the convergence rate  $\mathcal{O}(\epsilon^{-1})$  of the conjugate method provides a worst case instance that can be beaten in some applications with some suitable cost functions. From Eq. (67) we see that  $\epsilon = k^{-2}$  for learning arbitrary unitaries via the minimization of  $C_F$ , meaning that convergence is obtained with the faster rate  $\mathcal{O}(\epsilon^{-1/2})$ . On the other hand, there are no obvious simplifications for the optimization of the trace distance, since the latter still requires the diagonalization of Eq. (46). For the trace distance, or its smooth version, only numerical approaches are feasible.

## VII. TELEPORTATION PROCESSOR

One possible (shallow) design for the quantum processor  $Q$  is the teleportation protocol [44] which has to be applied to a generic program state  $\pi$  instead of a maximally entangled state. In dimension  $d$ , the program  $\pi^{AB}$  is a  $d \times d$  state. The teleportation protocol involves a basis of  $d^2$  maximally entangled states  $|\Phi_i\rangle$  and a basis  $\{U_i\}$  of teleportation unitary such that  $\text{Tr}(U_i^\dagger U_j) = d\delta_{ij}$  [45]. In the protocol, an input  $d$ -dimensional state  $\rho^S$  and the  $A$  part of the program  $\pi^{AB}$  are subject to the projector  $|\Phi_i\rangle\langle\Phi_i|$ . The classical outcome  $i$  is communicated to the  $B$  part of  $\pi^{AB}$  where the correction  $U_i^{-1}$  is applied. In this way, we implement the following teleportation channel  $\mathcal{E}_\pi$  from qudit  $S$  to qudit  $B$

$$\mathcal{E}_\pi(\rho) = \sum_i U_i^B \langle\Phi_i^{SA}| \rho^S \otimes \pi^{AB} |\Phi_i^{SA}\rangle U_i^{B\dagger}. \quad (68)$$

The Choi matrix of the teleportation channel  $\mathcal{E}_\pi$  can be written as  $\chi_\pi = \Lambda_{\text{tele}}(\pi)$ , where the map of the teleportation processor is equal to

$$\Lambda_{\text{tele}}(\pi) = \frac{1}{d^2} \sum_i (U_i^* \otimes U_i) \pi (U_i^* \otimes U_i)^\dagger. \quad (69)$$

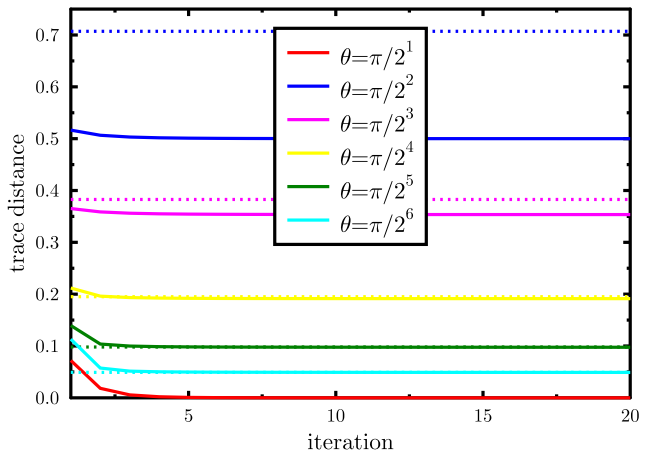


FIG. 3. Optimization of program states for simulating the rotation  $R(\theta) = e^{i\theta X}$  with a teleportation processor. The optimization is via the minimization of trace distance  $C_1$  of Eq. (9) with the projected subgradient method in Eq. (50). The dashed lines correspond to the upper bound  $\sqrt{1 - F[\Lambda(\tilde{\pi}_F), \chi_\epsilon]^2}$  of the trace distance, where  $\tilde{\pi}_F$  is the optimal program that maximizes the fidelity, namely the eigenvector of Eq. (64) with maximum eigenvalue.

Note that, if the program  $\pi$  is teleportation covariant [21], namely if  $[\pi, U_i^* \otimes U_i] = 0$ , then  $\pi$  is automatically a fixed point of the map, i.e., we have  $\chi_\pi := \Lambda_{\text{tele}}(\pi) = \pi$ . Also note that, the channel in Eq. (69) is self-dual, i.e.,  $\Lambda^* = \Lambda$ . As a result, for any operator  $\hat{O}$ , we may write

$$\Lambda_{\text{tele}}^*(\hat{O}) = \frac{1}{d^2} \sum_i (U_i^* \otimes U_i) \hat{O} (U_i^* \otimes U_i)^\dagger. \quad (70)$$

As an example, assume that the target channel is a unitary  $U$ , so that its Choi matrix is  $\chi_U := |\chi_U\rangle\langle\chi_U|$  with  $|\chi_U\rangle = \mathbb{1} \otimes U|\Phi\rangle$  and  $|\Phi\rangle$  is maximally entangled. By using Eq. (70) and  $U^* \otimes \mathbb{1}|\Phi\rangle = \mathbb{1} \otimes U^\dagger|\Phi\rangle$ , we may write the dual processor map

$$\begin{aligned} \Lambda_{\text{tele}}^* [|\chi_U\rangle\langle\chi_U|] &= \frac{1}{d^2} \sum_i (\mathbb{1} \otimes V_i^U) |\Phi\rangle\langle\Phi| (\mathbb{1} \otimes V_i^U)^\dagger, \end{aligned} \quad (71)$$

where  $V_i^U = U_i U U_i^\dagger$ . The maximum eigenvector of  $\Lambda_{\text{tele}}^* [|\chi_U\rangle\langle\chi_U|]$  represents the optimal program state  $\tilde{\pi}_F$  for simulating the unitary  $U$  via the teleportation processor (according to the fidelity cost function). In some cases, the solution is immediate. For instance, this happens when  $V_i^U \propto U$  is independent of  $i$ . This is the case when  $U$  is a teleportation unitary, because it satisfies the Weyl-Heisenberg algebra [21]. For a teleportation unitary  $U$ , we simply have

$$\Lambda^* [|\chi_U\rangle\langle\chi_U|] = |\chi_U\rangle\langle\chi_U|, \quad (72)$$

so that the unique optimal program is  $\tilde{\pi}_F = |\chi_U\rangle\langle\chi_U|$ .

In Fig. 3 we show the convergence of the projected subgradient algorithm using the teleportation processor

and target unitaries  $R(\theta) = e^{i\theta X}$ , for different values of  $\theta$ . When  $\theta$  is a multiple of  $\pi/2$ , then the above unitary is teleportation covariant and the Frank-Wolfe algorithm converges to zero trace distance. For other values of  $\theta$  perfect simulation is impossible, and we notice that the algorithm converges to a non zero value of the trace distance (9). For comparison, in Fig. 3 we also plot the value of the fidelity upper bound  $\sqrt{1 - F[\Lambda(\tilde{\pi}_F), \chi_{\mathcal{E}}]^2}$ , where  $\tilde{\pi}_F$  is the optimal program that maximizes the fidelity of Eq. (17), namely the eigenvector of Eq. (71) with maximum eigenvalue. We note that for  $\theta = \pi/2^\ell$  the trace distance decreases for larger  $\theta$ . The limit case  $\ell \rightarrow \infty$  is perfectly simulable as  $R(0)$  is teleportation covariant.

### A. Pauli channel simulation

Pauli channels are defined as [1]

$$\mathcal{P}(\rho) = \sum_i p_i U_i \rho U_i^\dagger, \quad (73)$$

where  $U_i$  are generalized Pauli operators and  $p_i$  some probabilities. For  $d = 2$  the Pauli operators are the four Pauli matrices  $I, X, Y, Z$  and in any dimension they form the Weyl-Heisenberg group [1]. These operators are exactly the teleportation unitaries  $U_j$  defined in the previous section. The Choi matrix  $\chi_{\mathcal{P}}$  of a Pauli channel  $\mathcal{P}$  is diagonal in the Bell basis, i.e., we have

$$\chi_{\mathcal{P}} = \sum_i p_i |\Phi_i\rangle\langle\Phi_i|, \quad (74)$$

where  $\Phi_i = \mathbb{1} \otimes U_i |\Phi\rangle$  and  $|\Phi\rangle = \sum_{j=1}^d |jj\rangle / \sqrt{d}$ .

We now consider the simulation of a Pauli channel with the teleportation quantum processor introduced in the previous section. Let

$$\pi = \sum_{ij} \pi_{ij} |\Phi_i\rangle\langle\Phi_j|, \quad (75)$$

be an arbitrary program state expanded in the Bell basis. For any program state, the Choi matrix of the teleportation-simulated channel is given by Eq. (69). Using standard properties of the Pauli matrices we find

$$\chi_{\pi} \equiv \Lambda(\pi) = \sum_i \pi_{ii} |\Phi_i\rangle\langle\Phi_i|, \quad (76)$$

namely a generic state is transformed into a Bell diagonal state. Therefore, the cost function

$$C_1^{\text{Pauli}} = \|\chi_{\mathcal{P}} - \chi_{\pi}\|_1, \quad (77)$$

can be minimized analytically for any Pauli channel by choosing  $\pi_{ij} = p_i \delta_{ij}$ . With this choice we find  $C_1^{\text{Pauli}} = 0$ , meaning that the simulation is perfect.

From theory [46–48] we know that only Pauli channels can be perfectly simulated in this way. No matter how more general we can make the states  $\pi$ , it is

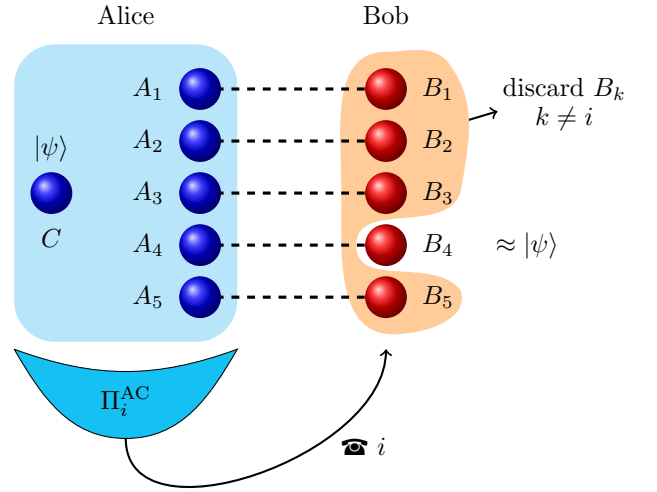


FIG. 4. PBT scheme. Two distant parties, Alice and Bob, share  $N$  maximally entangled pairs  $\{A_k, B_k\}_{k=1}^N$ . Alice also has another system  $C$  in the state  $|\psi\rangle$ . To teleport  $C$ , Alice performs the POVM  $\Pi_i^{AC}$  on all her local systems  $\mathbf{A} = \{A_k\}_{k=1}^N$  and  $C$ . She then communicates the outcome  $i$  to Bob. Bob discards all his systems  $\mathbf{B} = \{B_k\}_{k=1}^N$  with the exception of  $B_i$ . After these steps, the state  $|\psi\rangle$  is approximately teleported to  $B_i$ . Similarly, an arbitrary channel  $\mathcal{E}$  is simulated with  $N$  copies of the Choi matrix  $\chi_{\mathcal{E}}^{A_k B_k}$ . The figure shows an example with  $N = 5$ , where  $i = 4$  is selected.

proven [46, 47] that these are the only channels we can perfectly simulate. This is true even if we apply the Pauli corrections in a probabilistic way, i.e., we assume a classical channel from the Bell outcomes to the corresponding label of the Pauli correction operator [47].

## VIII. PORT-BASED TELEPORTATION

We now study a design of programmable quantum processor that can potentially simulate any target quantum channel in the asymptotic limit of an arbitrarily large program state. This design is PBT [11–13], a generalization of the standard teleportation scheme. For finite-dimensional programs, a PBT processor cannot achieve a perfect deterministic simulation of an arbitrary channel [10]. In this realistic finite-dimensional setting, our study finally establishes the optimal performance achievable by this type of quantum processor.

### A. Basics of PBT

The overall protocol of PBT is illustrated in Fig. 4. Unlike standard teleportation protocol, PBT requires that Alice and Bob share  $N$  entangled pairs for the simulation of the identity channel [11]. The protocol is based on a resource state (the program) given by  $\pi_{\mathbf{AB}} = \bigotimes_{k=1}^N \Phi_{A_k B_k}$ ,

where  $|\Phi_{A_k B_k}\rangle$  are Bell states for Alice's  $N$  qudits  $\mathbf{A} = (A_1, \dots, A_N)$  and Bob's  $N$  qudits  $\mathbf{B} = (B_1, \dots, B_N)$ . After preparing such a state, Alice performs a joint positive-operator value measure (POVM)  $\{\Pi_i\}$  on her  $\mathbf{A}$ -half of  $\pi_{\mathbf{AB}}$  and an input state  $|\psi\rangle_C$  that she wishes to teleport. She communicates the outcome  $i$  to Bob, who discards all "ports"  $\mathbf{B}$  except  $B_i = B_{\text{out}}$ . The resulting PBT channel  $\mathcal{P}_\pi : \mathcal{H}_C \mapsto \mathcal{H}_{B_{\text{out}}}$  is then

$$\begin{aligned} \mathcal{P}_\pi(\rho) &= \sum_{i=1}^N \text{Tr}_{\mathbf{A}\bar{\mathbf{B}}_i C} [\Pi_i(\pi_{\mathbf{AB}} \otimes \rho_C)]_{B_i \rightarrow B_{\text{out}}} \\ &= \sum_{i=1}^N \text{Tr}_{\mathbf{A}\bar{\mathbf{B}}_i C} \left[ \sqrt{\Pi_i}(\pi_{\mathbf{AB}} \otimes \rho_C) \sqrt{\Pi_i} \right]_{B_i \rightarrow B_{\text{out}}}, \end{aligned} \quad (78)$$

where  $\bar{\mathbf{B}}_i = \mathbf{B} \setminus B_i = \{B_k : k \neq i\}$ . In the limit  $N \rightarrow \infty$ , PBT approximates an identity channel  $\mathcal{P}_\pi(\rho) \approx \rho$ .

In the standard PBT protocol [11, 12] the following POVM is used

$$\Pi_i = \tilde{\Pi}_i + \frac{1}{N} \left( \mathbb{1} - \sum_k \tilde{\Pi}_k \right), \quad (79)$$

where

$$\tilde{\Pi}_i = \sigma_{\mathbf{AC}}^{-1/2} \Phi_{A_i C} \sigma_{\mathbf{AC}}^{-1/2}, \quad (80)$$

$$\sigma_{\mathbf{AC}} := \sum_{i=1}^N \Phi_{A_i C}, \quad (81)$$

and  $\sigma^{-1/2}$  is an operator defined only on the support of  $\sigma$ . The PBT protocol is formulated for  $N \geq 2$  ports. However, we also include here the trivial case for  $N = 1$ , corresponding to the process where Alice's input is traced out and the output is the reduced state of Bob's port, i.e., a maximally mixed state.

With the choice of the POVM in Eq. (79), the identity channel  $\mathcal{I}$  can be simulated with fidelity [11, 13]

$$F_\pi = 1 - \mathcal{O}\left(\frac{1}{N}\right), \quad (82)$$

so perfect simulation is possible only in the limit  $N \rightarrow \infty$ . More generally, it has been shown [14] that simulation error in diamond norm scales as

$$\|\mathcal{I} - \mathcal{P}_\pi\|_\diamond \leq \frac{2d(d-1)}{N}. \quad (83)$$

## B. Channel simulation via PBT

Any generic channel  $\mathcal{E}$  can be written as a composition  $\mathcal{E} \circ \mathcal{I}$  between  $\mathcal{E}$  and the identity channel  $\mathcal{I}$ . Channel simulation can be achieved by replacing the identity channel  $\mathcal{I}$  with its PBT simulation  $\mathcal{P}_\pi$ , and then applying  $\mathcal{E}$  to  $B_i$ . However, since Bob does not perform any post-processing on its systems  $\mathbf{B}$ , aside from discarding all ports  $B_k$  with  $k \neq i$ , he can also apply *first* the channel  $\mathcal{E}^{\otimes N}$  to all his

ports and *then* discard all the ports  $B_k$  with  $k \neq i$ . In doing so, he changes the program state to

$$\pi_{\mathbf{AB}} = \mathbb{1}_A \otimes \mathcal{E}_B^{\otimes N} \left[ \bigotimes_{k=1}^N \Phi_{A_k B_k} \right] = \bigotimes_{k=1}^N \chi_{\mathcal{E}}^{A_k B_k}. \quad (84)$$

In other terms, any channel  $\mathcal{E}$  can be PBT-approximated by  $N$  copies of its Choi matrix  $\chi_{\mathcal{E}}$  as program state. However, while such a program state is optimal when  $N \rightarrow \infty$ , for finite  $N$  there may be better alternatives. In general, for any finite  $N$ , finding the optimal program state  $\pi_{\mathbf{AB}}$  simulating a channel  $\mathcal{E}$  with PBT is an open problem, and no explicit solutions or procedures are known.

We employ our convex optimization procedures to find the optimal program state. This can be done either exactly by minimizing the diamond distance cost function  $C_\diamond$  via SDP, or approximately, by determining the optimal program state via the minimization of the trace distance cost function  $C_1$  via the gradient-based ML techniques discussed above. For this second approach, we need to derive the map  $\Lambda$  of the PBT processor, between the program state  $\pi$  to output Choi matrix as in Eq. (8). From the definition in Eq. (78) we find the following operator sum decomposition

$$\begin{aligned} \Lambda(\pi) &= \chi_{\mathcal{P}_\pi} = \mathbb{1}_D \otimes \mathcal{P}_\pi[\Phi_{DC}] \\ &= \sum_{i=1}^N \text{Tr}_{\mathbf{A}\bar{\mathbf{B}}_i C} \left[ \sqrt{\Pi_i}(\pi_{\mathbf{AB}} \otimes \Phi_{DC}) \sqrt{\Pi_i} \right]_{B_i \rightarrow B_{\text{out}}} \\ &= \sum_{ik} K_{ik} \pi K_{ik}^\dagger, \end{aligned} \quad (85)$$

where the corresponding Kraus operators are

$$K_{ik}^{\mathbf{AB} \rightarrow DB_{\text{out}}} = \langle e_k^{(i)} | \sqrt{\Pi_i} \otimes \mathbb{1}_{\mathbf{BD}} | \Phi_{DC} \rangle, \quad (86)$$

and  $|e_k^{(i)}\rangle$  span a basis of  $\mathbf{A}\bar{\mathbf{B}}_i C$ .

## C. Program state compression

The program state grows exponentially with the number of ports  $N$  as  $d^{2N}$  where  $d$  is the dimension of the Hilbert space. However, as also discussed in the original proposal [11, 12] and more recently in Ref. [49], the resource state of PBT can be chosen with extra symmetries, so as to reduce the number of free parameters. In particular, we may consider the set of program states that are symmetric under the exchange of ports, i.e., such that rearranging any  $A$  modes and the corresponding  $B$  modes leaves the program state unchanged.

Let  $P_s$  be the permutation operator swapping labels 1 to  $N$  for the labels in the sequence  $s$ , which contains all the numbers 1 to  $N$  once each in some permuted order. Namely  $P_s$  exchanges all ports according to the rule  $i \mapsto s_i$ . Since PBT is symmetric under exchange of ports, we may write

$$\mathcal{P}_{P_s \pi P_s^\dagger}(\rho) = \mathcal{P}_\pi(\rho) \text{ for any } s. \quad (87)$$

Consider then an arbitrary permutation-symmetric resource state  $\pi_{\text{sym}}$  as

$$\pi_{\text{sym}} = \frac{1}{N!} \sum_s P_s \pi P_s^\dagger,$$

where the sum is over all possible sequences  $s$  that define independent permutations and  $N!$  is the total number of possible permutations. Clearly  $\mathcal{P}_{\pi_{\text{sym}}} = \mathcal{P}_\pi$ , so any program state gives the same PBT channel as some symmetric program state. It therefore suffices to consider the set of symmetric program states. This is a convex set: any linear combination of symmetric states is a symmetric state.

To construct a basis of the symmetric space, we note that each element of a density matrix is the coefficient of a dyadic (of the form  $|x\rangle\langle y|$ ). If permutation of labels maps one dyadic to another, the coefficients must be the same. This allows us to constrain our density matrix using fewer global parameters. For instance, for  $d = 2$  we can define the 16 parameters  $n_{00,00}$ ,  $n_{00,01}$ ,  $n_{00,10}$ , etc., corresponding to the number of ports in the dyadic of the form  $|0_A 0_B\rangle\langle 0_A 0_B|$ ,  $|0_A 0_B\rangle\langle 0_A 1_B|$ ,  $|0_A 0_B\rangle\langle 1_A 0_B|$ , etc. Each element of a symmetric density matrix can then be defined solely in terms of these parameters, i.e., all elements corresponding to dyadics with the same values of these parameters have the same value.

For the general qudit case, in which our program state consists of  $N$  ports, each composed of two  $d$ -dimensional qudits, we can find the number of independent parameters from the number of independent dyadics. Each port in a dyadic can be written as  $|a_A, b_B\rangle\langle c_A, d_B|$  where the extra indices  $A$  and  $B$  describe whether those states are modeling either qudit  $A$  or  $B$ . There are  $d^4$  different combinations of  $\{a, b, c, d\}$ , so we can place each qudit into one of  $d^4$  categories based on these values. If two elements in the density matrix correspond to dyadics with the same number of ports in each category, they must take the same value. Hence, the number of independent coefficients is given by the number of ways of placing  $N$  (identical) ports into  $d^4$  (distinguishable) categories. This is exactly the binomial coefficient

$$\binom{N + d^4 - 1}{d^4 - 1} = \mathcal{O}(N^{d^4 - 1}). \quad (88)$$

Consequently, exploiting permutation symmetry of the PBT protocol, we can *exponentially* reduce the number of parameters for the optimization over program states.

The number of parameters can be reduced even further by considering products of Choi matrices. We may focus indeed on the Choi set

$$\mathcal{C}_N = \left\{ \pi : \pi = \sum_k p_k \chi_k^{\otimes N} \right\}, \quad (89)$$

where each  $\chi_k = \chi_{AB}^k$  is a generic Choi matrix, therefore satisfying  $\text{Tr}_B \chi_k = d^{-1} \mathbb{1}$ , and  $p_k$  form a probability distribution. Clearly  $\mathcal{C}$  is a convex set. We now show that this set can be further reduced to just considering  $N = 1$ .

When the program state  $\pi = \chi^{\otimes N}$  is directly used in Eq. (85) we find

$$\Lambda(\pi) = \sum_{i=1}^N \text{Tr}_{\mathbf{A}\bar{\mathbf{B}}_i C} [\Pi_i (\chi_{AB}^{\otimes N} \otimes \Phi_{DC})]_{B_i \rightarrow B_{\text{out}}} \quad (90)$$

$$= \frac{1}{d^{N-1}} \sum_{i=1}^N \text{Tr}_{A_i C} [\Pi_i (\chi_{A_i B_{\text{out}}} \otimes \Phi_{DC})] \quad (91)$$

$$:= \tilde{\Lambda}(\chi), \quad (92)$$

namely that the optimization can be reduced to the  $\mathcal{O}(d^4)$  dimensional space of Choi matrices  $\chi$ . Note that, in the above equation, we used the identity

$$\text{Tr}_{\bar{\mathbf{B}}_i} \chi_{AB}^{\otimes N} = \chi_{A_i B_i} \otimes \frac{\mathbb{1}_{\bar{\mathbf{A}}_i}}{d^{N-1}}, \quad (93)$$

where  $\bar{\mathbf{A}}_i = \mathbf{A} \setminus A_i$ .

Now let  $\pi$  be a linear combination of tensor products of Choi matrix states,  $\chi_k^{\otimes N}$ , each with probability  $p_k$  as in Eq. (89). Then we can write

$$\text{Tr}_{\bar{\mathbf{B}}_i} \pi_{AB} = \text{Tr}_{\bar{\mathbf{B}}_i} \sum_k p_k \chi_k^{\otimes N} \quad (94)$$

$$= \sum_k p_k \left( \chi_{A_i B_i}^k \otimes \frac{\mathbb{1}_{\bar{\mathbf{A}}_i}}{d^{N-1}} \right). \quad (95)$$

However, this is precisely the partial trace over the tensor product  $\chi'^{\otimes N}$  of some other Choi matrix  $\chi' = \sum_k p_k \chi_k$ . Hence, the program state  $\pi = \sum_k p_k \chi_k^{\otimes N}$  simulates the same channel as the resource state  $\pi' = (\sum_k p_k \chi_k)^{\otimes N}$ .

Therefore, the optimization over the convex set  $\mathcal{C}_N$  can be reduced to the optimization over products of Choi matrices  $\chi^{\otimes N}$ . From Eq. (92) this can be further reduced to the optimization of the quantum channel  $\tilde{\Lambda}$  over the convex set of single-copy Choi matrices  $\chi$

$$\mathcal{C}_1 = \{ \pi : \pi = \chi_{AB}, \text{Tr}_B \chi_{AB} = \mathbb{1}/2 \}, \quad (96)$$

which is  $\mathcal{O}(d^4)$ . Using  $\mathcal{C}_1$  drastically reduces the difficulty of numerical simulations, thus allowing the exploration of significantly larger values of  $N$ . Details on how to explicitly construct  $\tilde{\Lambda}$  for  $d = 2$  are presented in Appendix C.

## D. Numerical examples

We first consider the simulation of an amplitude damping channel  $\mathcal{E}_{\text{AD}}(\rho) = \sum_i K_i^{\text{AD}} \rho K_i^{\text{AD}\dagger}$ , which is defined by the Kraus operators

$$K_0^{\text{AD}} = \begin{pmatrix} 1 & 0 \\ 0 & \sqrt{1-p} \end{pmatrix}, \quad K_1^{\text{AD}} = \begin{pmatrix} 0 & \sqrt{p} \\ 0 & 0 \end{pmatrix}. \quad (97)$$

In Fig. 5 we study the performance of the PBT simulation of the amplitude damping channel  $\mathcal{E}_{\text{AD}}$  for different choices of  $p$ . For  $p = 0$  the amplitude damping is equal to

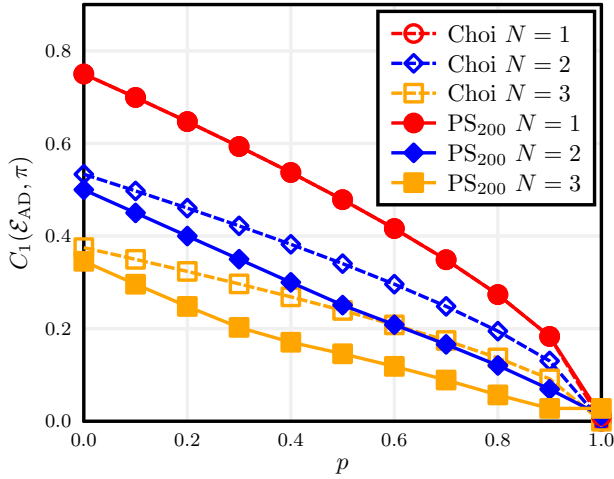


FIG. 5. PBT Simulation of the amplitude damping channel  $\mathcal{E}_{\text{AD}}$  for various damping rates  $p$ . Minimization of the trace distance  $C_1(\mathcal{E}_{\text{AD}}, \pi) = \|\chi_{\mathcal{E}_{\text{AD}}} - \chi_\pi\|_1$  between the target channel’s Choi matrix and its PBT simulation with program state  $\pi$ , for different number of ports  $N$ . We consider  $N = 1, 2, 3$  and two kinds of programs: copies of the channel’s Choi matrix  $\chi_{\mathcal{E}_{\text{AD}}}^{\otimes N}$  and the state  $\tilde{\pi}_1$  obtained from the minimization of  $C_1$  via the projected subgradient (PS) method after 200 iterations. Note that the simulation error  $C_1$  is maximum for the identity channel ( $p = 0$ ) and goes to zero for  $p \rightarrow 1$ .

the identity channel, while for  $p = 1$  it is a “reset” channel sending all states to  $|0\rangle$ . We compare the simulation error with program states  $\pi$  either made by products of the channel’s Choi matrix  $\chi_{\mathcal{E}_{\text{AD}}}^{\otimes N}$  as in Eq. (84) or obtained from the minimization of the trace distance cost function of Eq. (9) with the projected subgradient iteration in Eq. (50). Alternative methods, like the conjugated gradient algorithm, perform similarly for this channel. We observe that, surprisingly, the optimal program  $\tilde{\pi}_1$  obtained by minimizing the trace distance  $C_1$  is always better than the natural choice  $\chi_{\mathcal{E}_{\text{AD}}}^{\otimes N}$ .

In Fig. 6 we study the PBT simulation of the amplitude damping channel by considering the subset of program states  $\pi = \chi^{\otimes N}$  which is made of tensor products of the  $4 \times 4$  generic Choi matrices  $\chi$  (therefore satisfying  $\text{Tr}_2 \chi = \mathbb{1}/2$ ). As discussed in previous Sec. VIII C, this is equivalent to optimizing over the Choi set  $\mathcal{C}_N$  and it practically reduces to the convex optimization of the channel  $\tilde{\Lambda}$  over the generic single-copy Choi matrix  $\chi$ . Moreover,  $\tilde{\Lambda}$  itself can be simplified, as shown in Appendix C, so the all operations depend polynomially on the number  $N$  of ports. This allows us to numerically explore much larger values of  $N$ , even for the minimization of  $C_\diamond$ . In Fig. 6 the dotted lines correspond to the value of  $C_\diamond$  when the program  $\pi = \chi_{\mathcal{E}_{\text{AD}}}^{\otimes N}$  is employed, where  $\chi_{\mathcal{E}_{\text{AD}}}$  is the channel’s Choi matrix. As Fig. 6 shows, the cost  $C_\diamond$  may be significantly smaller with an optimal  $\chi$ , thus showing that the optimal program may be different from the channel’s Choi matrix, especially when  $p$  is far from the two boundaries  $p = 0$  and  $p = 1$ .

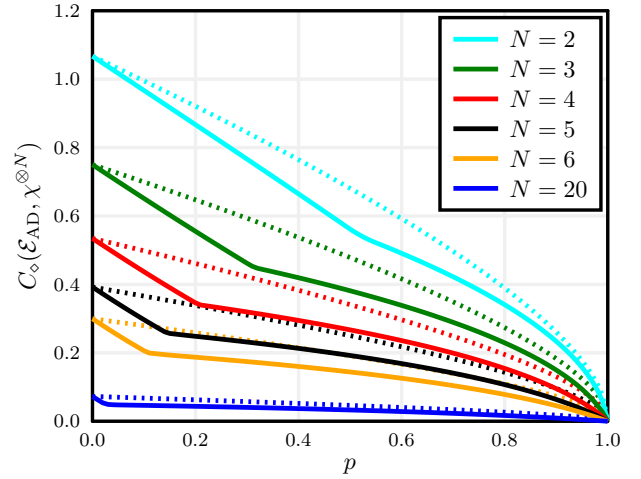


FIG. 6. PBT Simulation of the amplitude damping channel  $\mathcal{E}_{\text{AD}}$  for various damping rates  $p$ . We plot the diamond distance cost function  $C_\diamond(\mathcal{E}_{\text{AD}}, \pi) = \|\mathcal{E}_{\text{AD}} - \mathcal{E}_{\text{AD}, \pi}\|_\diamond$  between the target channel  $\mathcal{E}_{\text{AD}}$  and its PBT simulation  $\mathcal{E}_{\text{AD}, \pi}$  with program state  $\pi$ . In particular, for the program state we compare the naive choice of the channel’s Choi matrix  $\pi = \chi_{\mathcal{E}_{\text{AD}}}^{\otimes N}$  (dotted lines) with the SDP minimization over the set of generic Choi matrices  $\pi = \chi^{\otimes N}$  (solid lines). Different values of  $N = 2, \dots, 6$  and  $N = 20$  are shown.

As an another example, we consider the simulation of the depolarizing channel defined by

$$\mathcal{E}_{\text{dep}}(\rho) = (1 - p)\rho + \frac{p}{d}\mathbb{1}. \quad (98)$$

In Fig. 7 we study the performance of PBT simulation of the depolarizing channel in terms of  $p$ . For  $p = 0$  the depolarizing channel is equal to the identity channel, while for  $p = 1$  it sends all states to the maximally mixed state. Again we compare the simulation error with program states either made copies of the channel’s Choi matrices  $\chi_{\mathcal{E}_{\text{dep}}}^{\otimes N}$  or obtained from the minimization of  $C_1$  with the conjugate gradient method of Eq. (57), which performs significantly better than the projected subgradient for this channel. Also for the depolarizing channel we observe that, for any finite  $N$ , we obtain a lower error by optimizing over the program states instead of the naive choice  $\chi_{\mathcal{E}_{\text{dep}}}^{\otimes N}$ .

Finally, in Fig. 8 we study the PBT simulation of a unitary gate  $U_\theta = e^{i\theta X}$  for different values of  $\theta$ . Unlike the previous non-unitary channels, in Fig. 8 we observe a flat error where different unitaries have the same simulation error of the identity channel  $\theta = 0$ . This is expected because both the trace distance and the diamond distance are invariant under unitary transformations. In general, we have the following.

**Proposition 5** *Given a unitary  $\mathcal{U}(\rho) = U\rho U^\dagger$  and its PBT simulation  $\mathcal{U}_\pi$  with program  $\pi$  we may write*

$$\min_\pi \|\mathcal{U} - \mathcal{U}_\pi\|_\diamond = \min_\pi \|\mathcal{I} - \mathcal{I}_\pi\|_\diamond, \quad (99)$$

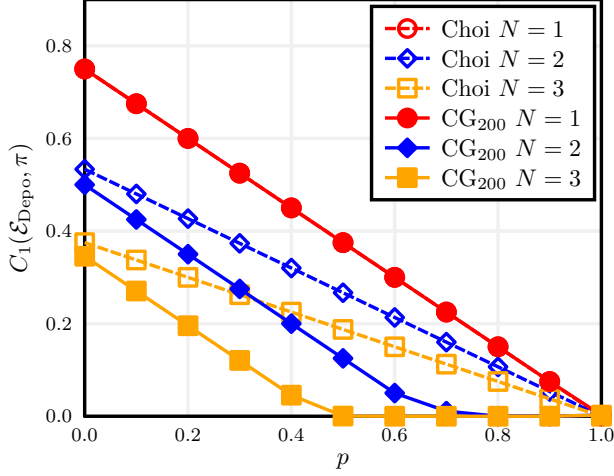


FIG. 7. PBT Simulation of the qubit depolarizing channel versus probability of depolarizing  $p$ . Trace distance  $C_1(\mathcal{E}_{\text{dep}}, \pi) = \|\chi_{\mathcal{E}_{\text{dep}}} - \chi_\pi\|_1$  between the target channel's Choi matrix and its PBT simulation with program state  $\pi$ , for different number of ports  $N$ . We consider  $N = 1, 2, 3$  and two kinds of programs: copies of the channel's Choi matrix  $\pi = \chi_{\mathcal{E}_{\text{dep}}}^{\otimes N}$  and the optimal program state  $\tilde{\pi}_1$  obtained from the minimization of  $C_1$  via the conjugate gradient (CG) method after 200 iterations. Note that the simulation error  $C_1$  is maximum for the identity channel ( $p = 0$ ) and eventually goes to zero for a finite value of  $p$  that decreases for increasing  $N$ .

where  $\mathcal{I}_\pi$  is the PBT simulation of the identity channel.

*Proof.* In fact, we simultaneously prove

$$\min_{\pi} \|\mathcal{I} - \mathcal{I}_\pi\|_{\diamond} \stackrel{(1)}{\leq} \min_{\pi} \|\mathcal{U} - \mathcal{U}_\pi\|_{\diamond} \stackrel{(2)}{\leq} \min_{\pi} \|\mathcal{I} - \mathcal{I}_\pi\|_{\diamond}, \quad (100)$$

where (1) comes from the fact that  $\|\mathcal{U} - \mathcal{U}_\pi\|_{\diamond} = \|\mathcal{U}^{-1}\mathcal{U} - \mathcal{U}^{-1}\mathcal{U}_\pi\|_{\diamond} = \|\mathcal{I} - \mathcal{U}^{-1}\mathcal{U}_\pi\|_{\diamond}$  and  $\mathcal{U}^{-1}\mathcal{U}_\pi$  is a possible PBT simulation of the identity  $\mathcal{I}$  with program state  $\mathcal{I} \otimes (\mathcal{U}^{-1})^{\otimes N}(\pi)$  once  $\mathcal{U}^{-1}$  is swapped with the filtering of the ports; then (2) comes from the fact that the composition  $\mathcal{U} \circ \mathcal{I}_\pi$  is a possible simulation of the unitary  $\mathcal{U}$  with program state  $\mathcal{I} \otimes \mathcal{U}^{\otimes N}(\pi)$  and we have the inequality  $\|\mathcal{U} \circ \mathcal{I} - \mathcal{U} \circ \mathcal{I}_\pi\|_{\diamond} \leq \|\mathcal{I} - \mathcal{I}_\pi\|_{\diamond}$ . ■

The scaling of  $\|\mathcal{I} - \mathcal{I}_\pi\|_{\diamond}$  for different values of  $N$  is plotted in Fig. 9 where numerical values are obtained from SDP, while the upper bound is given by Eq. (83).

## IX. PARAMETRIC QUANTUM CIRCUITS

We now study another design of universal quantum processor that can simulate any target quantum channel in the asymptotic limit of an arbitrarily large program state. This is based on a suitable reformulation of the PQCs, which are known to simulate any quantum computation with a limited set of quantum gates [20, 50].

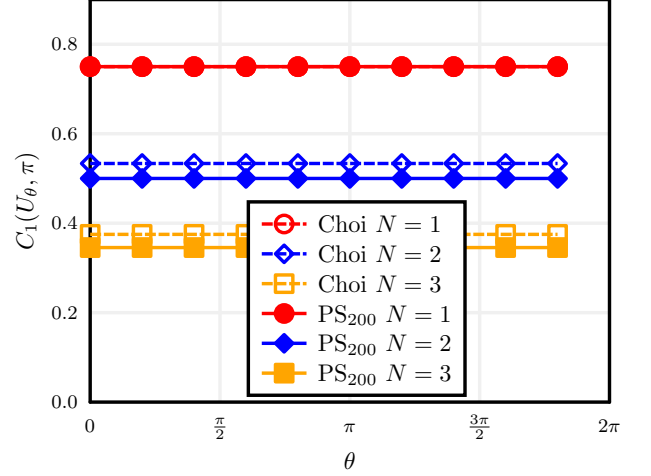


FIG. 8. PBT Simulation of the unitary gate  $U_\theta = e^{i\theta X}$  for different angles  $\theta$ , where  $X$  is the bit-flip Pauli matrix. Trace distance  $C_1(U_\theta, \pi) = \|\chi_{U_\theta} - \chi_\pi\|_1$  between the target Choi matrix of the unitary and its PBT simulation with program state  $\pi$ , for different number of ports  $N$ . We consider  $N = 1, 2, 3$  and two kinds of programs: copies of the Choi matrix of the unitary  $\chi_{U_\theta}^{\otimes N}$  and the program state  $\tilde{\pi}_1$  obtained from the minimization of  $C_1$  via the projected subgradient (PS) method after 200 iterations.

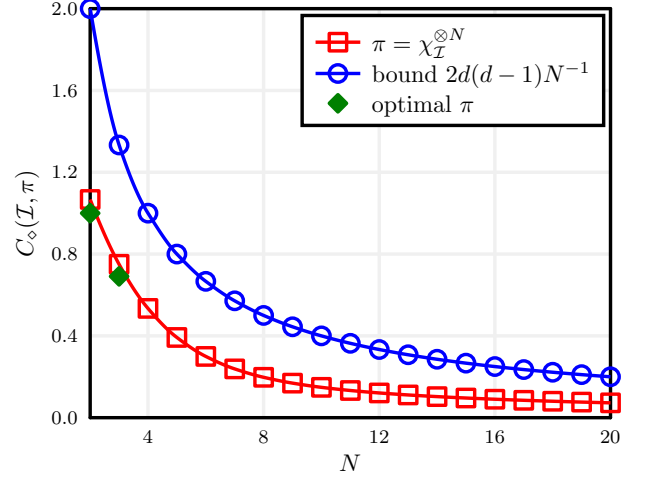


FIG. 9. PBT Simulation of the identity channel for different number of ports  $N$ . For the identity channel the optimal Choi matrix coincides with the channel's Choi matrix  $\chi_{\mathcal{I}}$ . The optimal  $\pi$  has been obtained by minimising  $C_o$  via SDP. The upper bound corresponds to Eq. (83).

### A. Basic idea

A PQC is composed of a sequence of unitary matrices  $U_j(\theta_j)$ , each depending on a classical parameter  $\theta$ . The resulting unitary operation is then

$$U(\theta) = U_N(\theta_N) \dots U_2(\theta_2) U_1(\theta_1). \quad (101)$$

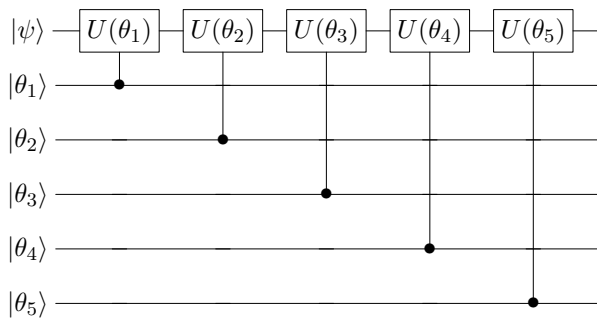


FIG. 10. Convex reformulation of a PQC as a coherent programmable quantum processor that applies a sequence of conditional gates as in Eq. (102) depending on the program state  $|\pi\rangle = |\theta_1, \dots, \theta_N\rangle$ . The program state is not destroyed and can be reused.

A convenient choice is via  $U_j(\theta_j) = \exp(i\theta_j H_j)$ , where each elementary gate corresponds to a Schrödinger evolution with Hamiltonian  $H_j$  for a certain time interval  $\theta_j$ . For certain choices of  $H_j$  and suitably large  $N$  the above circuit is universal [20], namely any unitary can be obtained with  $U(\theta)$  and a suitable choice of  $\theta_j$ . The optimal parameters can be found with numerical algorithms [51], e.g. by minimizing the cost function  $C(\theta) = |\text{Tr}[U_{\text{target}}^\dagger U(\theta)]|$ . However, the above cost function is not convex, so the numerical algorithms are not guaranteed to converge to the global optimum.

As a first step, we show that the task of learning the optimal parameters in a PQC can be transformed into a convex optimization problem by using a quantum program. This allows us to use SDP and gradient-based ML methods for finding the global optimum solution.

### B. Convex reformulation

Consider a program state  $|\pi\rangle = |\theta_1, \dots, \theta_N\rangle$  composed by  $N$  registers  $R_j$ , each in a separable state  $|\theta_j\rangle$ . We can transform the classical parameters in Eq. (101) into quantum parameters via the conditional gates

$$\hat{U}_j = \exp\left(iH_j \otimes \sum_{\theta_j} \theta_j |\theta_j\rangle\langle\theta_j|\right), \quad (102)$$

that acts non-trivially on system and register  $R_j$ . If the parameters  $\theta_j$  are continuous, then we can replace the sum with an integral. With the above gates we define the parametric quantum channel

$$Q_\pi(\rho) = \text{Tr}_R \left[ \prod_{j=1}^N \hat{U}_j (\rho \otimes \pi) \prod_{j=1}^N \hat{U}_j^\dagger \right], \quad (103)$$

whose action on a generic state  $|\psi\rangle$  is shown in Fig. 10. For a pure separable program  $|\pi\rangle = |\theta_1, \dots, \theta_N\rangle$ , we obtain the standard result, i.e.,

$$Q_{|\theta_1, \dots, \theta_N\rangle}(\rho) = U(\theta)\rho U(\theta)^\dagger, \quad (104)$$

where  $U(\theta)$  is defined in Eq. (101). The parametric quantum processor  $Q_\pi$  in Eq. (103) is capable of simulating any parametric quantum channels, but it is more general, as it allows entangled quantum parameters and also parameters in quantum superposition.

An equivalent measurement-based protocol is obtained by performing the trace in Eq. (109) over the basis  $|\theta_1, \dots, \theta_N\rangle$ , so that

$$Q_\pi(\theta) = \sum_{\{\theta_j\}} U(\theta)\rho U(\theta)^\dagger \langle\theta_1, \dots, \theta_N|\pi|\theta_1, \dots, \theta_N\rangle, \quad (105)$$

where  $U(\theta)$  is defined in Eq. (101). In this alternative, yet equivalent formulation, at a certain iteration  $j$ , the processor measures the qubit register  $R_j$ . Depending on the measurement outcome  $\theta_j$ , the processor then applies a different unitary  $U(\theta_j)$  on the system. However, in this formulation the program state  $|\pi\rangle$  is destroyed after each channel use. From Eq. (105) we note that  $Q_\pi$  depends on  $\pi$  only via the probability distribution  $\langle\theta_1, \dots, \theta_N|\pi|\theta_1, \dots, \theta_N\rangle$ . As such any advantage in using quantum states can only come from the capability of quantum systems to model computationally hard probability distributions [52].

### C. Universal channel simulation via PQCs

The universality of PQCs can be employed for universal channel simulation. Indeed, thanks to Stinespring's dilation theorem, any channel can be written as a unitary evolution on a bigger space, where the system is paired to an extra register  $R_0$

$$\mathcal{E}(\rho_A) = \text{Tr}_{R_0}[U(\rho_A \otimes \theta_0)U^\dagger], \quad (106)$$

where  $\theta_0$  belongs to  $R_0$ , and  $U$  acts on system  $A$  and register  $R_0$ . In Ref. [50] it was shown that two quantum gates are universal for quantum computation. Specifically, given  $U_0 = e^{it_0 H_0}$  and  $U_B = e^{it_1 H_1}$  for fixed times  $t_i$  and Hamiltonians  $H_j$ , it is possible to write any unitary as

$$U \approx \dots U_1^{m_4} U_0^{m_3} U_1^{m_2} U_0^{m_1}, \quad (107)$$

for some integers  $m_j$ . Under suitable conditions, it was shown that with  $M = \sum_j m_j = \mathcal{O}(d^2 \epsilon^{-d})$  it is possible to approximate any unitary  $U$  with a precision  $\epsilon$ . More precisely, the conditions are the following

- i) The Hamiltonians  $H_0$  and  $H_1$  are generators of the full Lie algebra, namely  $H_0, H_1$  and their repeated commutators generate all the elements of  $\text{su}(d)$ .
- ii) The eigenvalues of  $U_0$  and  $U_1$  have phases that are irrationally related to  $\pi$ .

The decomposition in Eq. (107) is a particular case of Eq. (101) where  $\theta_j$  can only take binary values  $\theta_j = 0, 1$ .

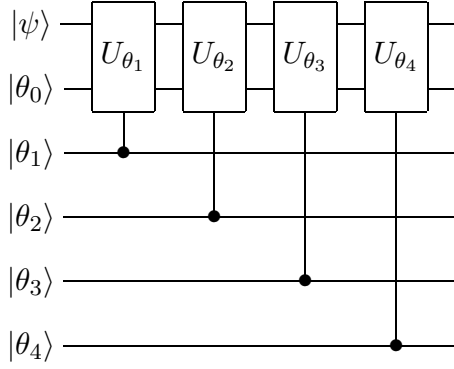


FIG. 11. Simulation of a quantum channel via Stinespring decomposition together with unitary simulation as in Fig. 10.

As such we can write the conditional gates of Eq. (102) as

$$\hat{U}_j = \exp(it_0 H_0 \otimes |0\rangle_{jj}\langle 0| + it_1 H_1 \otimes |1\rangle_{jj}\langle 1|), \quad (108)$$

for some times  $t_j$ . Channel simulation is then obtained by replacing the unitary evolution  $U$  of Eq. (106) with the approximate form in Eq. (107) and its simulation in Eq. (109). The result is illustrated in Fig. 11 and described by the following channel

$$Q_\pi(\rho) = \text{Tr}_{\mathbf{R}} \left[ \prod_{j=1}^N \hat{U}_{jA,R_0,R_j} (\rho_A \otimes \pi) \prod_{j=1}^N \hat{U}_{jA,R_0,R_j}^\dagger \right], \quad (109)$$

where the program state  $\pi$  is defined over  $\mathbf{R} = (R_0, \dots, R_N)$  and each  $\hat{U}_j$  acts on the input system  $A$  and two ancillary qubits  $R_0$  and  $R_j$ . The decomposition of Eq. (107) assures that, with the program

$$|\pi\rangle = |\theta_0\rangle \otimes \dots \otimes |1\rangle^{\otimes m_2} \otimes |0\rangle^{\otimes m_1}, \quad (110)$$

the product of unitaries approximates  $U$  in Eq. (106) with precision  $\epsilon$ . This is possible in general, provided that the program state has dimension  $\mathcal{O}(d^2 \epsilon^{-d})$ . However, the channel (109) is more general, as it allows both quantum superposition and entanglement.

The processor map  $\Lambda$  is then simply obtained as

$$\Lambda(\pi) = \text{Tr}_{\mathbf{R}} \left[ \hat{U}_{\mathbf{AR}} (\Phi_{BA} \otimes \pi_{\mathbf{R}}) \hat{U}_{\mathbf{AR}}^\dagger \right], \quad (111)$$

where

$$\hat{U}_{\mathbf{AR}} = \mathbb{1}_B \otimes \prod_{j=1}^N \hat{U}_{jA,R_0,R_j}, \quad (112)$$

while the (non-trace-preserving) dual channel may be written as

$$\Lambda^*(X) = \langle \Phi_{BA} | \hat{U}_{\mathbf{AR}}^\dagger (X_{BA} \otimes \mathbb{1}_{\mathbf{R}}) \hat{U}_{\mathbf{AR}} | \Phi_{BA} \rangle. \quad (113)$$

This channel requires  $2N$  quantum gates at each iteration and can be employed for the calculation of gradients,

following Theorem 2. When we are interested in simulating a unitary channel  $U$  via the quantum fidelity, then following the results of Section VI, the corresponding optimal program  $\tilde{\pi}_F$  is simply the eigenvector  $\Lambda^*[|\chi_U\rangle\langle\chi_U|]$  with maximum eigenvalue, where  $|\chi_U\rangle = \mathbb{1} \otimes U|\Phi\rangle$ . Note also that  $\Lambda^*[|\chi_U\rangle\langle\chi_U|] = Z^\dagger Z$  where

$$Z = (\langle\chi_U|_{BA} \otimes \mathbb{1}_{\mathbf{R}}) \hat{U}_{\mathbf{AR}} (|\Phi_{BA}\rangle \otimes \mathbb{1}_{\mathbf{R}}), \quad (114)$$

so the optimal program  $\tilde{\pi}_F$  is the principal component of  $Z$ . Since there are quantum algorithms for principal component analysis [53], the optimization may be efficiently performed on a quantum computer.

#### D. Numerical examples

As an example we study the simulation of an amplitude damping channel, with Kraus operators in Eq. (97). A possible Stinespring dilation for this channel is obtained with  $|\theta_0\rangle = |0\rangle$  and

$$U = \begin{pmatrix} 1 & 0 & 0 & 0 \\ 0 & \sqrt{1-p} & \sqrt{p} & 0 \\ 0 & -\sqrt{p} & \sqrt{1-p} & 0 \\ 0 & 0 & 0 & 1 \end{pmatrix} = e^{iH_{\text{AD}}}, \quad (115)$$

where the Hamiltonian is given by

$$H_{\text{AD}} = \frac{\arcsin(\sqrt{p})}{2} (Y \otimes X - X \otimes Y), \quad (116)$$

with  $X$  and  $Y$  being Pauli operators. We may construct a PQC simulation by taking

$$U_0 = e^{i\alpha(Y \otimes X - X \otimes Y)}, \quad (117)$$

for some  $\alpha$  and taking  $U_1$  to be a different unitary that makes the pair  $U_0, U_1$  universal. Here we may choose  $\alpha = \sqrt{2}$  and  $U_1 = e^{iH_1}$  with

$$H_1 = (\sqrt{2}Z + \sqrt{3}Y + \sqrt{5}X) \otimes (Y + \sqrt{2}Z). \quad (118)$$

Results are shown in Fig. 12. Compared with the similar PBT simulation of Fig. 5, we observe that PQC simulation displays a non-monotonic behavior as a function of  $N$ . PBT with  $N$  pairs requires a register of  $2N$  qubits, while PQC requires  $N+1$  qubits, namely  $N$  qubits from the conditional gates and an extra one coming from Stinespring decomposition (see Fig. 11). We observe that, with a comparable yet finite register size, PQC can outperform PBT in simulating the amplitude damping channel. In Fig. 13 we also study the PQC simulation of the depolarizing channel for different values of  $p$ . Although the gates  $U_0$  and  $U_1$  were chosen with inspiration from the Stinespring decomposition of the amplitude damping channel, those gates are universal and capable of simulating other channels. Indeed, we observe in Fig. 13 that a depolarizing channel is already well simulated with  $N=4$  for all values of  $p$ .

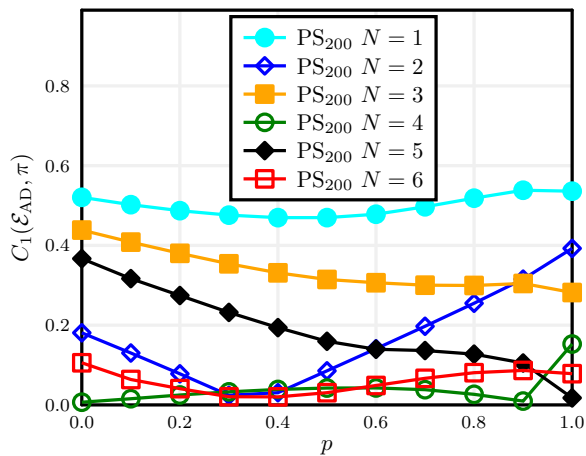


FIG. 12. PQC simulation of the amplitude damping channel. Trace distance  $C_1(\mathcal{E}_{\text{AD}}, \pi) = \|\chi_{\mathcal{E}_{\text{AD}}} - \chi_\pi\|_1$  between the target channel's Choi matrix and its PQC simulation with program state  $\pi$ , for different numbers of register qubits  $N$ . The optimal program is obtained from the minimization of  $C_1$  via the projected subgradient (PS) method after 200 iterations.

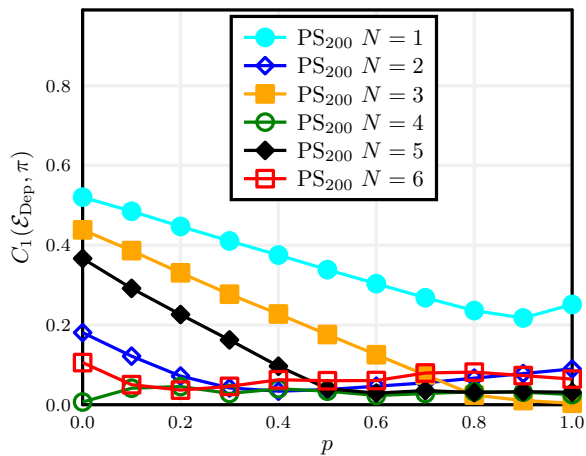


FIG. 13. PQC simulation of the depolarizing channel. Trace distance  $C_1(\mathcal{E}_{\text{Dep}}, \pi) = \|\chi_{\mathcal{E}_{\text{Dep}}} - \chi_\pi\|_1$  between the target channel's Choi matrix and its UPQC simulation with program state  $\pi$ , for different numbers of register qubits  $N$ . The optimal program is obtained from the minimization of  $C_1$  via the projected subgradient (PS) method after 200 iterations.

## X. CONCLUSIONS

In this work we have considered a general, finite-dimensional, model of programmable quantum processor, which is a fundamental scheme for quantum computing and also a primitive tool for other areas of quantum information. By introducing suitable cost functions, based on the diamond distance, trace distance and quantum fidelity, we have shown how to characterize the optimal performance of this processor in the simulation of an arbitrary quantum gate or channel. In fact, we have shown that the minimization of these cost functions is a convex

optimization problem that can always be solved.

In particular, by minimizing the diamond distance via SDP, we can always determine the optimal program state for the simulation of an arbitrary channel. Alternatively, we may minimize the simpler but larger cost functions in terms of trace distance and quantum fidelity via gradient-based ML methods, so as to provide a very good approximation of the optimal program state. This other approach can also provide closed analytical solutions, as is the case for the simulation of arbitrary unitaries, for which the minimization of the fidelity cost function corresponds to compute an eigenvector.

We have then applied our results to various designs of programmable quantum processor, from a shallow teleportation-based scheme to deeper and asymptotically-universal designs that are based on PBT and PQCs. We have explicitly benchmarked the performances of these quantum processors by considering the simulation of unitary gates, depolarizing and amplitude damping channels, showing that the optimal program states may differ from the naive choice based on the Choi matrix of the target channel.

An immediate application of our work may be the development of a model of “programmable” blind quantum computation, where a client has an input state to be processed by a quantum server which is equipped with a programmable quantum processor. The client classically informs the server about what type of computation it needs (e.g., some specified quantum algorithm) and the server generates an optimal program state which closely approximates the overall quantum channel to be applied to the input. The server then accepts the input from the client, processes it, and returns the output together with the value of a cost function quantifying how close the computation was with respect to the client's request.

Our results may also be useful in areas beyond quantum computing, wherever channel simulation is a basic problem. For instance this is the case of quantum communication, for the derivation of quantum and private communication capacities, and quantum metrology and hypothesis testing, for the simplification of adaptive protocols and the analysis of the ultimate discrimination and estimation performance with quantum channels.

**Acknowledgements.** L.B. acknowledges support by the program “Rita Levi Montalcini” for your young researchers. S.P. acknowledges support by the EPSRC via the ‘UK Quantum Communications Hub’ (EP/M013472/1) and the European Union via the project ‘Continuous Variable Quantum Communications’ (CiViQ, no 820466). S.P. would like to thank George Zweig, Jacques Carolan, John Watrous, and Dirk Englund for discussions and feedback.

## Appendix A: Matrix calculus

### 1. Matrix differentiation

For a general overview of these techniques, the reader may consult Ref. [54]. Thanks to Cauchy's theorem, a matrix function can be written as

$$f(A) = \frac{1}{2\pi i} \int_{\Gamma} d\lambda f(\lambda)(\lambda\mathbb{1} - A)^{-1}. \quad (\text{A1})$$

For the same reason

$$f'(A) = \frac{1}{2\pi i} \int_{\Gamma} d\lambda f(\lambda)(\lambda\mathbb{1} - A)^{-2}. \quad (\text{A2})$$

Applying a basic rule of matrix differentiation,  $d(A^{-1}) = -A^{-1}(dA)A^{-1}$  we obtain

$$df(A) = \frac{1}{2\pi i} \int_{\Gamma} d\lambda f(\lambda)(\lambda\mathbb{1} - A)^{-1}dA(\lambda\mathbb{1} - A)^{-1}. \quad (\text{A3})$$

Clearly,  $df(A) = f'(A)dA$  only when  $[A, dA] = 0$ . In general  $df(A)$  is a superoperator that depends on  $A$  and is applied to  $dA$ . The explicit form is easily computed using the eigenvalue decomposition or other techniques [54]. Note that in some cases the expressions are simple. Indeed, using the cyclic invariance of the trace, we have

$$d\text{Tr}[f(A)] = \text{Tr}[f'(A)dA], \quad (\text{A4})$$

while in general  $d\text{Tr}[Bf(A)] \neq \text{Tr}[Bf'(A)dA]$ .

### 2. Differential of the quantum fidelity

The quantum fidelity can be expanded as

$$\begin{aligned} F(X, Y) &= \text{Tr}\sqrt{\sqrt{X}Y\sqrt{X}} \\ &= \frac{1}{2\pi i} \int_{\Gamma} d\lambda \sqrt{\lambda} \text{Tr}[(\lambda\mathbb{1} - \sqrt{X}Y\sqrt{X})^{-1}], \end{aligned} \quad (\text{A5})$$

where in the second line we have applied Eq. (A1). Taking the differential with respect to  $Y$  and using the cyclic property of the trace we get

$$\begin{aligned} d_Y F &:= F(X, Y + dY) - F(X, Y) \\ &\stackrel{(1)}{=} \frac{1}{2\pi i} \int_{\Gamma} d\lambda \sqrt{\lambda} \text{Tr}[(\lambda\mathbb{1} - \sqrt{X}Y\sqrt{X})^{-2} \sqrt{X}dY\sqrt{X}] \\ &\stackrel{(2)}{=} \frac{1}{2} \text{Tr}[(\sqrt{X}Y\sqrt{X})^{-\frac{1}{2}} \sqrt{X}dY\sqrt{X}] \\ &\stackrel{(3)}{=} \frac{1}{2} \text{Tr}[\sqrt{X}(\sqrt{X}Y\sqrt{X})^{-\frac{1}{2}} \sqrt{X}dY], \end{aligned} \quad (\text{A6})$$

where in (1) we use Eq. (A3) and the cyclic property of the trace; in (2) we use Eq. (A2) with  $f(\lambda) = \sqrt{\lambda}$ , so  $f'(\lambda) = \frac{1}{2}\lambda^{-1/2}$ ; and in (3) we use the cyclic property of the trace. See also Lemma 11 in [35].

### 3. Differential of the trace distance

The trace norm for a Hermitian operator  $X$  is defined as

$$\begin{aligned} t(X) &= \|X\|_1 := \text{Tr}\sqrt{X^\dagger X} = \text{Tr}[\sqrt{X^2}] \\ &= \frac{1}{2\pi i} \int_{\Gamma} d\lambda \sqrt{\lambda} \text{Tr}[(\lambda\mathbb{1} - XX)^{-1}], \end{aligned} \quad (\text{A7})$$

where in the second line we applied Eq. (A1). From the spectral decomposition  $X = U\lambda U^\dagger$  we find  $t(X) = \sum_j |\lambda_j|$ , so the trace distance reduces to the absolute value function for one-dimensional Hilbert spaces. The absolute value function  $|\lambda|$  is differentiable at every points, except  $\lambda = 0$ . Therefore, for any  $\lambda \neq 0$  the subgradient of the absolute value function is made by its gradient, namely

$$\partial|\lambda| = \{\text{sign}(\lambda)\} \quad \text{for } \lambda \neq 0. \quad (\text{A8})$$

For  $\lambda = 0$  we can use the definition (34) to write

$$\partial|\lambda|_{\lambda=0} = \{z : |\sigma| \geq z\sigma \text{ for all } \sigma\}, \quad (\text{A9})$$

which is true iff  $-1 \leq z \leq 1$ . Therefore,

$$\partial|\lambda|_{\lambda=0} = [-1, 1]. \quad (\text{A10})$$

The sign function in (A8) can be extended to  $\lambda = 0$  in multiple ways (common choices are  $\text{sign}(0) = -1, 0, 1$ ). From the above equation, it appears that for any extension of the sign function, provided that  $\text{sign}(0) \in [-1, 1]$  we may write the general form

$$\text{sign}(\lambda) \in \partial|\lambda|, \quad (\text{A11})$$

which is true for any value of  $\lambda$ .

With the same spirit we extend the above argument to any matrix dimension, starting from the case where  $X$  is an invertible operator (no zero eigenvalues). Taking the differential with respect to  $X$  we find

$$\begin{aligned} dt(X) &:= t(X + dX) - t(X) = \\ &\stackrel{(1)}{=} \frac{1}{2\pi i} \int_{\Gamma} d\lambda \sqrt{\lambda} \text{Tr}[(\lambda\mathbb{1} - X^2)^{-2}(X(dX) + (dX)X)] \\ &\stackrel{(2)}{=} \frac{1}{2} \text{Tr}[(X^2)^{-\frac{1}{2}}(X(dX) + (dX)X)] \\ &\stackrel{(3)}{=} \text{Tr}[(X^2)^{-\frac{1}{2}}X(dX)] \end{aligned} \quad (\text{A12})$$

where in (1) we use Eq. (A3), the cyclic property of the trace and the identity  $dX^2 = X(dX) + (dX)X$ ; in (2) we use Eq. (A2) with  $f(\lambda) = \sqrt{\lambda}$ , so  $f'(\lambda) = \frac{1}{2}\lambda^{-1/2}$ ; and in (3) we use the cyclic property of the trace and the commutation of  $X$  and  $\sqrt{X^2}$ . Let

$$X = \sum_k \lambda_k P_k, \quad (\text{A13})$$

be the eigenvalue decomposition of  $X$  with eigenvalues  $\lambda_k$  and eigenprojectors  $P_k$ . For non-zero eigenvalues we may write

$$(X^2)^{-\frac{1}{2}}X = \sum_k \text{sign}(\lambda_k)P_k =: \text{sign}(X), \quad (\text{A14})$$

and accordingly

$$\begin{aligned} dt(X) &:= \|X + dX\|_1 - \|X\|_1 \\ &= \sum_k \text{sign}(\lambda_k)\text{Tr}[P_k dX]. \end{aligned} \quad (\text{A15})$$

Therefore, for invertible operators we may write

$$\partial t(X) = \{\nabla t(X)\}, \quad \nabla t(X) = \text{sign}(X).$$

We now consider the general case where some eigenvalues of  $X$  may be zero. We do this by generalizing Eq. (A11), namely we show that even if  $\partial t(X)$  may contain multiple elements, it is always true that  $\nabla t \in \partial t$ , provided that  $-\mathbf{1} \leq \text{sign}(X) \leq \mathbf{1}$ . Following (34) we may write, for fixed  $X$  and arbitrary  $Y$ ,

$$\begin{aligned} &t(Y) - t(X) - \text{Tr}[\nabla t(X)(Y - X)] \\ &\stackrel{(1)}{=} t(Y) - t(X) - \text{Tr}[\nabla t(X)Y] + t(X) \\ &\stackrel{(2)}{\geq} t(Y) - \text{Tr}[Y] = \sum_j (|\lambda_j| - \lambda_j) \geq 0, \end{aligned} \quad (\text{A16})$$

where in (1) we use the property  $\|X\|_1 = \text{Tr}[\text{sign}(X)X]$  and in (2) we use the assumption  $-\mathbf{1} \leq \text{sign}(X) \leq \mathbf{1}$ . From the definition of the subgradient (34), the above equation shows that  $\text{sign}(X) \in \partial t(X)$ , so we may always use  $\nabla t(X) = \text{sign}(X)$  in the projected subgradient algorithm (50).

## Appendix B: Smoothing techniques

### 1. Stochastic smoothing

The conjugate gradient algorithm converges after  $\mathcal{O}(c/\epsilon)$  steps [16, 17], where  $\epsilon$  is the desired precision and  $c$  is a curvature constant that depends on the function. However, it is known that  $c$  could diverge for non-smooth functions. This is the case for the trace norm, as shown in Example 0.1 in [55].

A general solution, valid for arbitrary functions, is via stochastic smoothing [56]. In this approach the non-smooth function  $C(\pi)$  is replaced by the average

$$C_\eta(\pi) = \mathbb{E}_\sigma[C(\pi + \eta\sigma)]. \quad (\text{B1})$$

where  $\sigma$  is such that  $\|\sigma\|_\infty \leq 1$ . If  $|C(x) - C(y)| \leq M\|x - y\|_\infty$ , then

$$C(\pi) \leq C_\eta(\pi) \leq C(\pi) + M\eta, \quad (\text{B2})$$

so that  $C_\eta(\pi)$  provides a good approximation for  $C(\pi)$ . Moreover,  $C_\eta$  is differentiable at any point, so we may apply the conjugate gradient algorithm. A modified conjugate gradient algorithm with adaptive stochastic approximation was presented in Ref. [57], At each iteration  $k$  the algorithm reads

- 1) Sample some operators  $\sigma_1, \dots, \sigma_k$ ,
- 2) Evaluate  $\bar{g}_k = \frac{1}{k} \sum_{j=1}^k g(\pi_k + \eta_k \sigma_j)$  for  $\eta_k \propto k^{-1/2}$ ,
- 3) Find the smallest eigenvalue  $|\sigma_k\rangle$  of  $\bar{g}_k$ ,
- 4)  $\pi_{k+1} = \frac{k}{k+2}\pi_k + \frac{2}{k+2}|\sigma_k\rangle\langle\sigma_k|$ .

where  $g$  denotes any element of the subgradient  $\partial C$ . The above algorithm converges after  $\mathcal{O}(\epsilon^2)$  iterations. Since Eqs. (40) and (38) provide an element of the subgradient, the above algorithm can be applied to both fidelity and trace distance. However, this algorithm requires  $k$  evaluation of the subgradient to perform the averages, so it may be impractical when the number of iterations get larger. In the following we study an alternative that does not require any average.

### 2. Nesterov's smoothing

An alternative smoothing scheme is based on Nesterov's dual formulation [38]. Suppose that the non-smooth objective function  $f$  admits a dual representation as follows

$$f(x) = \sup_y [\langle x, y \rangle - g(y)], \quad (\text{B3})$$

for some inner product  $\langle \cdot, \cdot \rangle$ . Nesterov's approximation consists in adding a strongly convex function  $d$  to the dual

$$f_\mu(x) = \sum_y [\langle x, y \rangle - g(y) - \mu d(y)]. \quad (\text{B4})$$

The resulting  $\mu$ -approximation is smooth and satisfies

$$f_\mu(x) \leq f(x) \leq f_\mu(x) + \mu \sup_y d(y). \quad (\text{B5})$$

The trace norm admits the dual representation [25]

$$t(X) = \|X\|_1 = \sup_{\|Y\|_\infty \leq 1} \langle Y, X \rangle, \quad (\text{B6})$$

where  $\langle Y, X \rangle$  is the Hilbert Schmidt product. This can be regularized with any strongly convex function  $d$ . A convenient choice [19] that enables an analytic solution is via  $d(X) = \frac{1}{2}\|X\|_2^2 := \frac{1}{2}\langle X, X \rangle$  so

$$t_\mu(X) = \max_{\|Y\|_\infty \leq 1} \left[ \langle Y, X \rangle - \frac{\mu}{2}\|Y\|_2^2 \right]. \quad (\text{B7})$$

This function is smooth and its gradient is given by [19]

$$\begin{aligned} \nabla t_\mu(X) &= \operatorname{argmax}_{\|Y\|_\infty \leq 1} \left[ \langle Y, X \rangle - \frac{\mu}{2}\|Y\|_2^2 \right] \\ &= \operatorname{argmin}_{\|Y\|_\infty \leq 1} \|\mu Y - X\|_2^2 = U \Sigma_\mu V^\dagger, \end{aligned}$$

where  $X = U\Sigma V^\dagger$  is the singular value decomposition of  $X$  and  $\Sigma_\mu$  is a diagonal matrix with diagonal entries  $(\Sigma_\mu)_i = \min\{\Sigma_i/\mu, 1\}$ . Plugging this into Eq. (B7) we get

$$t_\mu(X) = \text{Tr} \left[ \Sigma_\mu \left( \Sigma - \frac{\mu}{2} \Sigma_\mu \right) \right]. \quad (\text{B8})$$

For a diagonalizable matrix  $X$  with spectral decomposition  $X = U\lambda U^\dagger$ , the singular value decomposition is obtained with  $\Sigma = |\lambda|$  and  $V = U\text{sign}(\lambda)$ . Inserting these expressions in (B8) we find

$$t_\mu(X) = \sum_j h_\mu(\lambda_j) = \text{Tr}[h_\mu(X)], \quad (\text{B9})$$

where  $h_\mu$  is the so called Huber penalty function

$$h_\mu(x) = \begin{cases} \frac{x^2}{2\mu} & \text{if } |x| < \mu, \\ |x| - \frac{\mu}{2} & \text{if } |x| \geq \mu. \end{cases} \quad (\text{B10})$$

The gradient  $\nabla t_\mu$  is then  $h'_\mu(X) \equiv U h'(\lambda) U^\dagger$ , where

$$h'_\mu(x) = \begin{cases} \frac{x}{\mu} & \text{if } |x| < \mu, \\ \text{sign}(x) & \text{if } |x| \geq \mu. \end{cases} \quad (\text{B11})$$

We find then that via the smooth trace norm  $t_\mu$  we can define the smooth trace distance of Eq. (59) that is differentiable at every point

$$C_\mu(\pi) = \text{Tr} [h_\mu(\chi_\pi - \chi_\mathcal{E})]. \quad (\text{B12})$$

Thanks to the inequalities in (B5), the smooth trace distance bounds the cost  $C_1$  as

$$C_\mu(\pi) \leq C_1(\pi) \leq C_\mu(\pi) + \frac{\mu d}{2}, \quad (\text{B13})$$

where we employed the identity  $\sup_{\|Y\|_\infty \leq 1} \|Y\|_2^2 \leq d$  to get the upper bound. Moreover, we find the following

**Lemma 6** *The smooth trace distance, defined in Eq. (59), is a convex function of  $\pi$ .*

*Proof.* From the definition and Eq. (B7) we find

$$\begin{aligned} C_\mu(\pi) &= t_\mu[\Lambda(\pi) - \chi_\mathcal{E}] \\ &= \max_{\|Y\|_\infty \leq 1} \left[ \langle Y, \Lambda(\pi) - \chi_\mathcal{E} \rangle - \frac{\mu}{2} \|Y\|_2^2 \right]. \end{aligned} \quad (\text{B14})$$

Now for  $\bar{\pi} = p\pi_1 + (1-p)\pi_2$  linearity implies  $f(\bar{\pi}) := \langle Y, \Lambda(\bar{\pi}) - \chi_\mathcal{E} \rangle = pf(\pi_1) + (1-p)f(\pi_2)$ . Therefore

$$\begin{aligned} C_\mu(\bar{\pi}) &= \max_{\|Y\|_\infty \leq 1} \left[ pf(\pi_1) + (1-p)f(\pi_2) - \frac{\mu}{2} \|Y\|_2^2 \right] \\ &\leq p \max_{\|Y\|_\infty \leq 1} \left[ \langle Y, \Lambda(\pi_1) - \chi_\mathcal{E} \rangle - \frac{\mu}{2} \|Y\|_2^2 \right] \\ &\quad + (1-p) \max_{\|Z\|_\infty \leq 1} \left[ \langle Z, \Lambda(\pi_2) - \chi_\mathcal{E} \rangle - \frac{\mu}{2} \|Z\|_2^2 \right] \\ &= pC_\mu(\pi_1) + (1-p)C_\mu(\pi_2), \end{aligned} \quad (\text{B15})$$

showing the convexity. ■

Then, using the definitions from [38], the following theorem bounds on the growth of the gradient

**Theorem 7** *The gradient of the smooth trace norm is Lipschitz continuous with Lipschitz constant*

$$L = \frac{d}{\mu}. \quad (\text{B16})$$

In particular, being the gradient Lipschitz continuous, the smooth trace norm satisfies the following inequality for any state  $\pi, \sigma$

$$C_\mu(\sigma) \leq C_\mu(\pi) + \langle \nabla C_\mu(\pi), \sigma - \pi \rangle + \frac{L}{2} \|\sigma - \pi\|_2^2. \quad (\text{B17})$$

*Proof.* Given the linearity of the quantum channel  $\Lambda$ , we can apply theorem 1 from [38] to find

$$L = \frac{1}{\mu} \sup_{\|x\|_2=1, \|y\|_2=1} \langle y, \Lambda(x) \rangle. \quad (\text{B18})$$

Since all eigenvalues of  $y$  are smaller or equal to 1, we can write  $y \leq \mathbb{1}$  and as such

$$L \leq \frac{1}{\mu} \sup_{\|x\|_2=1} \text{Tr}[\Lambda(x)] = \frac{1}{\mu} \sup_{\|x\|_2=1} \text{Tr}[x] \leq \frac{d}{\mu}. \quad (\text{B19})$$

■

### Appendix C: PBT reduced channel

Here we provide an explicit expression for the reduced map  $\tilde{\Lambda}$  of Eq. (92) in the case of qubits. For  $d = 2$  we can rewrite PBT in a language that can be more easily formulated from representations of  $\text{SU}(2)$ . For simplicity of notation, here we do not use bold letters for vectorial quantities.

Let us modify the POVM in Eq. (78) as

$$\tilde{\Pi}_i = \sigma_{AC}^{-1/2} \Psi_{A_i C}^- \sigma_{AC}^{-1/2}, \quad (\text{C1})$$

$$\sigma_{AC} = \sum_{i=1}^N \Psi_{A_i C}^-, \quad (\text{C2})$$

$$\Pi_i = \tilde{\Pi}_i + \Delta, \quad (\text{C3})$$

$$\Delta = \frac{1}{N} \left( \mathbb{1} - \sum_j \tilde{\Pi}_j \right), \quad (\text{C4})$$

where  $|\Psi^- \rangle = (|01\rangle - |10\rangle)/\sqrt{2}$  is a singlet state. For  $\pi = \chi^{\otimes n}$  the quantum channel is simplified. In fact, since  $\text{Tr}_B \chi = \mathbb{1}/2$ , we may write

$$\begin{aligned} \mathcal{P}_\pi &= \sum_{i=1}^N \frac{1}{2^{N-1}} \text{Tr}_{AC} \left[ \sqrt{\tilde{\Pi}_i} (\rho_C \otimes \chi_{A_i B} \otimes \mathbb{1}_{\bar{A}_i}) \sqrt{\tilde{\Pi}_i} \right] \\ &= \sum_{\ell} K_\ell^0 (\rho_C \otimes \chi) K_\ell^{0\dagger} + \sum_{\ell'} K_{\ell'}^1 (\rho_C \otimes \chi) K_{\ell'}^{1\dagger}, \end{aligned} \quad (\text{C5})$$

where  $\ell$  and  $\ell'$  are multi-indices and, in defining the Kraus operators, we have separated the contributions from  $\tilde{\Pi}_i$  and  $\Delta$  (see below).

In order to express these operators, we write

$$|\psi_{\bar{C}A_i}^-\rangle\langle\psi_{\bar{C}A_i}^-| = \frac{\mathbb{1} - \vec{\sigma}_C \cdot \vec{\sigma}_{A_i}}{4}, \quad (\text{C6})$$

so that

$$\begin{aligned} \sigma_{AC} &= \sum_{i=1}^N |\psi_{\bar{C}A_i}^-\rangle\langle\psi_{\bar{C}A_i}^-| = \frac{N}{4} - \vec{S}_C \cdot \vec{S}_A \\ &= \frac{N}{4} - \frac{\vec{S}_{\text{tot}}^2 - \vec{S}_C^2 - \vec{S}_A^2}{2}, \end{aligned} \quad (\text{C7})$$

where  $\vec{S} = \vec{\sigma}/2$  is a vector of spin operators,  $\vec{S}_A = \sum_j \vec{S}_{A_j}$  and  $\vec{S}_{\text{tot}} = \vec{S}_C + \vec{S}_A$ . The eigenvalues of  $\sigma_{AC}$  are then obtained from the eigenvalues of the three commuting Casimir operators

$$\lambda(s_A) = \frac{N}{4} - \frac{S_{\text{tot}}(S_{\text{tot}} + 1) - s_A(s_A + 1) - 3/4}{2}, \quad (\text{C8})$$

where  $S_{\text{tot}} = s_A \pm 1/2$ .

Substituting the definition of  $S_{\text{tot}}$ , we find two classes of eigenvalues

$$\lambda^+(s_A) = \frac{N - 2s_A}{4}, \quad \lambda^-(s_A) = \frac{N + 2s_A + 2}{4}, \quad (\text{C9})$$

with corresponding eigenvectors

$$|\pm, s_A, M, \alpha\rangle = \sum_{k,m} \Gamma_{s_A \pm \frac{1}{2}, s_A}^{M,m,k} |k\rangle_C |s_A, m, \alpha\rangle_A, \quad (\text{C10})$$

where  $-\frac{N+1}{2} \leq M \leq \frac{N+1}{2}$ ,  $\alpha = 1, \dots, g^{[N]}(s)$  describes the degeneracy,  $g^{[N]}(s)$  is the size of the degenerate subspace, and

$$\Gamma_{S,s}^{M,m,k} = \langle S, M; s, 1/2 | 1/2, 1/2 - k; s, m \rangle \quad (\text{C11})$$

are Clebsch-Gordan coefficients.

Note that the Clebsch-Gordan coefficients define a unitary transformation between the two bases  $|s_1, m_1; s_2, m_2\rangle$  and  $|S, M; s_1, s_2\rangle$ . From the orthogonality relations of these coefficients we find the equalities

$$\sum_{S,M} \Gamma_{S,s}^{M,m,i} \Gamma_{S,s}^{M,m',i'} = \delta_{i,i'} \delta_{m,m'}, \quad (\text{C12})$$

$$\sum_{m,i} \Gamma_{S,s}^{M,m,i} \Gamma_{S',s}^{M',m,i} = \delta_{M,M'} \delta(S, S', s), \quad (\text{C13})$$

where  $\delta(S, S', s) = 1$  iff  $S = S'$  and  $|s - 1/2| \leq S \leq s + 1/2$ . The eigenvalues in Eq. (C9) are zero iff  $S_{\text{tot}} = S_A + 1/2$  and  $S_A = N/2$ . These eigenvalues have degeneracy  $2S_{\text{tot}} + 1 = N + 2$  and the corresponding eigenvectors are

$$|\perp, M, \alpha\rangle = |+, N/2, M, \alpha\rangle. \quad (\text{C14})$$

Thus, the operator  $\Delta$  from Eq. (C4) may be written as

$$\Delta = \frac{1}{N} \sum_{M=-\frac{N+1}{2}}^{\frac{N+1}{2}} \sum_{\alpha} |\perp, M, \alpha\rangle\langle\perp, M, \alpha|. \quad (\text{C15})$$

To finish the calculation we need to perform the partial trace over all spins except those in port  $i$ . We use  $s_{\bar{A}_i}$ ,  $m_{\bar{A}_i}$  and  $\alpha_i$  to model the state of the total spin in ports  $A_j$  with  $j \neq i$ . These refer to the value of total spin and the projection along the  $z$  axis, as well as the degeneracy. Moreover, since  $S_{\bar{A}_i}^z$  commutes with both  $S_A^2$  and  $S_A^z$ , we may select a basis for the degeneracy that explicitly contains  $s_{\bar{A}_i}$ . We may write then  $\alpha = (s_{\bar{A}_i}, \tilde{\alpha}_i)$  where  $\tilde{\alpha}_i$  represents some other degrees of freedom.

With the above definitions, when we insert several resolutions of the identity in Eq. (C5), we may write the Kraus operators as

$$\begin{aligned} K_{i,s_{\bar{A}_i},m_{\bar{A}_i},\alpha_i,s'_{\bar{A}_i},m'_{\bar{A}_i},\alpha'_i}{}^0 &= 2^{-\frac{N-1}{2}} \langle s_{\bar{A}_i}, m_{\bar{A}_i}, \alpha_i | \otimes \langle \psi_{\bar{A}_i C}^- | \sigma_{AC}^{-1/2} | s'_{\bar{A}_i}, m'_{\bar{A}_i}, \alpha'_i \rangle \\ &= 2^{-\frac{N-1}{2}} \sum_{\pm, s_A, M, \alpha} \lambda_{\pm}(s_A)^{-1/2} \langle \psi_{\bar{A}_i C}^- | \langle s_{\bar{A}_i}, m_{\bar{A}_i}, \alpha_i | \pm, s_A, M, \alpha \rangle \langle \pm, s_A, M, \alpha | s'_{\bar{A}_i}, m'_{\bar{A}_i}, \alpha'_i \rangle, \\ K_{i,M,\alpha,s'_{\bar{A}_i},m'_{\bar{A}_i},\alpha'_i}{}^1 &= 2^{-\frac{N-1}{2}} N^{-1/2} \langle +, N/2, M, \alpha | s'_{\bar{A}_i}, m'_{\bar{A}_i}, \alpha'_i \rangle, \end{aligned} \quad (\text{C16})$$

where each set of states  $|s_{\bar{A}_i}, m_{\bar{A}_i}, \alpha_i\rangle$  represent a basis of the space corresponding to all ports  $j$  with  $j \neq i$ . To

simplify the Kraus operators we study the overlap

$$\begin{aligned} &\langle s_{\bar{i}}, m_{\bar{i}}, \alpha_i | \pm, S, M, \alpha \rangle \\ &= \sum_{k,m} |k\rangle_C \langle s_{\bar{i}}, m_{\bar{i}}, \alpha_i | \Gamma_{S \pm \frac{1}{2}, S}^{M,m,k} |S, m, \alpha\rangle_A \\ &= \sum_{k,m} |k\rangle_C \langle s_{\bar{i}}, m_{\bar{i}}, \alpha_i | \Gamma_{S \pm \frac{1}{2}, S}^{M,m,k} \sum_{\ell} |\ell\rangle_i |s'_{\bar{i}}, m'_{\bar{i}}, \alpha'_i\rangle_i \Gamma_{S, s'_{\bar{i}}}^{m, m'_{\bar{i}}, k} \\ &= \sum_{k,\ell,m} |k\rangle_C |\ell\rangle_A \Gamma_{S \pm \frac{1}{2}, S}^{M,m,k} \Gamma_{S, s'_{\bar{i}}}^{m, m_{\bar{i}}, \ell} \equiv \hat{Q}_{\pm, s, M}^{s_{\bar{i}}, m_{\bar{i}}}. \end{aligned} \quad (\text{C17})$$

In the last line we find that the overlap is independent on  $\alpha$  and  $\alpha_i$ , though with constraints  $\alpha = (s_{\bar{i}}, \alpha_i)$ , which requires  $\alpha_i = \alpha'_i$ . Therefore, different Kraus operators provide exactly the same operation and, accordingly, we can sum over these equivalent Kraus operators to reduce

the number of indices. After this process we get

$$\begin{aligned} K_{\ell}^0 &\equiv K_{s_{\bar{i}}, m_{\bar{i}}, m'_{\bar{i}}}^0 \\ &= 2^{-\frac{N-1}{2}} \sqrt{N} \sum_{\pm, s_A, M} \lambda_{\pm}(s_A)^{-1/2} \sqrt{g^{[N-1]}(s_{\bar{i}})} \times \\ &\quad \times \left( \langle \psi_{AC}^- | \hat{Q}_{\pm, s_A, M}^{s_{\bar{i}}, m_{\bar{i}}} \hat{Q}_{\pm, s_A, M}^{s_{\bar{i}}, m'_{\bar{i}}} \rangle \right) \otimes \mathbb{1}_B, \end{aligned} \quad (C18)$$

$$\begin{aligned} K_{\ell}^1 &\equiv K_{M, s_{\bar{i}}, m_{\bar{i}}}^1 \\ &= \sqrt{\frac{g^{[N-1]}(s_{\bar{i}})}{2^{N-1}}} \hat{Q}_{+, N/2, M}^{s_{\bar{i}}, m'_{\bar{i}}} \dagger \otimes \mathbb{1}_B. \end{aligned} \quad (C19)$$

The Kraus operators of the reduced channel  $\tilde{\Lambda}$  are obtained as  $(K_{\ell}^u \otimes \mathbb{1}_D)(|\Psi_{CD}^- \rangle \otimes \mathbb{1}_{AB})$ . It is simple to check that the above operators define a CPTP-map.

- 
- [1] M. A. Nielsen and I. L. Chuang, *Quantum Computation and Quantum Information* (Cambridge University Press, Cambridge, 2000).
- [2] C. M. Bishop, *Pattern Recognition and Machine Learning* (Springer, 2006).
- [3] P. Wittek, *Quantum Machine Learning: What Quantum Computing Means to Data Mining* (Academic Press, Elsevier, 2014).
- [4] J. Biamonte, P. Wittek, N. Pancotti, P. Rebentrost, N. Wiebe, and S. Lloyd, “Quantum machine learning,” *Nature (London)* **549**, 195 (2017).
- [5] V. Dunjko and H. J. Briegel, “Machine learning & artificial intelligence in the quantum domain: a review of recent progress,” *Rep. Prog. Phys.* **81**, 074001 (2018).
- [6] M. Schuld, I. Sinayskiy, and F. Petruccione, “An introduction to quantum machine learning,” *Contemporary Physics* **56**, 172–185 (2015).
- [7] C. Ciliberto, M. Herbster, Alessandro D. Ialongo, M. Pontil, A. Rocchetto, S. Severini, and L. Wossnig, “Quantum machine learning: a classical perspective,” *Proceedings of the Royal Society A: Mathematical, Physical and Engineering Sciences* **474**, 20170551 (2018).
- [8] E Tang, “A quantum-inspired classical algorithm for recommendation systems,” preprint arXiv:1807.04271 (2018).
- [9] E Tang, “Quantum-inspired classical algorithms for principal component analysis and supervised clustering,” preprint arXiv:1811.00414 (2018).
- [10] M. A. Nielsen and I. L. Chuang, “Programmable quantum gate arrays,” *Phys. Rev. Lett.* **79**, 321 (1997).
- [11] S. Ishizaka and T. Hiroshima, “Asymptotic teleportation scheme as a universal programmable quantum processor,” *Phys. Rev. Lett.* **101**, 240501 (2008).
- [12] S. Ishizaka and T. Hiroshima, “Quantum teleportation scheme by selecting one of multiple output ports,” *Phys. Rev. A* **79**, 042306 (2009).
- [13] S. Ishizaka, “Some remarks on port-based teleportation,” preprint arXiv:1506.01555 (2015).
- [14] S. Pirandola, R. Laurenza, and C. Lupo, “Fundamental limits to quantum channel discrimination,” preprint arXiv:1803.02834 (2018).
- [15] S. Boyd, L. Xiao, and A. Mutapcic, *Subgradient methods* (2003).
- [16] M. Jaggi, “Convex optimization without projection steps,” preprint arXiv:1108.1170 (2011).
- [17] M. Jaggi, “Revisiting frank-wolfe: projection-free sparse convex optimization,” in *Proceedings of the 30th International Conference on International Conference on Machine Learning - Volume 28* (JMLR. org, 2013) pp. 1–427.
- [18] J. Duchi, S. Shalev-Shwartz, Y. Singer, and T. Chandra, “Efficient projections onto the l1-ball for learning in high dimensions,” in *Proceedings of the 25th international conference on Machine learning* (ACM, 2008) pp. 272–279.
- [19] J. Liu, P. Musialski, P. Wonka, and J. Ye, “Tensor completion for estimating missing values in visual data,” *IEEE transactions on pattern analysis and machine intelligence* **35**, 208–220 (2013).
- [20] S Lloyd, “Universal quantum simulators,” *Science* **273**, 1073–1078 (1996).
- [21] S. Pirandola, R. Laurenza, C. Ottaviani, and L. Banchi, “Fundamental limits of repeaterless quantum communications,” *Nat. Commun.* **8**, 15043 (2017).
- [22] S. Pirandola, S. L. Braunstein, R. Laurenza, C. Ottaviani, T. P. W. Cope, G. Spedalieri, and L. Banchi, “Theory of channel simulation and bounds for private communication,” *Quant. Sci. Tech.* **3**, 035009 (2018).
- [23] J. Watrous, *The theory of quantum information* (Cambridge Univ. Press, 2018) freely available at <https://cs.uwaterloo.ca/~watrous/TQI/>.
- [24] A. Y. Kitaev, A. Shen, and M. N. Vyalyi, *Classical and quantum computation*, 47 (American Mathematical Society, Providence, Rhode Island, 2002) sec. 11.
- [25] J. Watrous, *Advanced Topics in Quantum Information Processing* (Lecture notes, 2004).
- [26] E. Knill, R. Laflamme, and G. J. Milburn, “A scheme for efficient quantum computation with linear optics,” *Nature* **409**, 46 (2001).
- [27] J. Watrous, “Simpler semidefinite programs for completely bounded norms,” *Chicago Journal of Theoretical Computer Science* **8**, 1–19 (2013).
- [28] C. A. Fuchs and J. van de Graaf, “Cryptographic distinguishability measures for quantum-mechanical states,” *IEEE Trans. Info. Theory* **45**, 1216–1227 (1999).

- [29] M. S. Pinsker, *Information and information stability of random variables and processes* (Holden-Day, San Francisco, 1964).
- [30] E. A. Carlen and E. H. Lieb, “Bounds for entanglement via an extension of strong subadditivity of entropy,” *Lett. Math. Phys.* **101**, 1–11 (2012).
- [31] A. Uhlmann, “The transition probability...” *Rep. Math. Phys.* **9**, 273–279 (1976).
- [32] John Watrous, “Semidefinite programs for completely bounded norms,” *Theory of Computing* **5**, 217–238 (2009).
- [33] I. Nechita, Z. Puchała, L. Paweła, and K. Życzkowski, “Almost all quantum channels are equidistant,” *J. Math. Phys.* **59**, 052201 (2018).
- [34] Y. Nesterov, *Introductory lectures on convex optimization: A basic course*, Vol. 87 (Springer Science & Business Media, New York, 2013).
- [35] B. Coutts, M. Girard, and J. Watrous, “Certifying optimality for convex quantum channel optimization problems,” preprint arXiv:1810.13295 (2018).
- [36] J. Duchi, E. Hazan, and Y. Singer, “Adaptive subgradient methods for online learning and stochastic optimization,” *Journal of Machine Learning Research* **12**, 2121–2159 (2011).
- [37] D. Garber and E. Hazan, “Faster rates for the frank-wolfe method over strongly-convex sets,” in *Proceedings of the 32nd International Conference on International Conference on Machine Learning-Volume 37* (JMLR.org, 2015) pp. 541–549.
- [38] Y. Nesterov, “Smooth minimization of non-smooth functions,” *Mathematical programming* **103**, 127–152 (2005).
- [39] R. Bhatia, *Matrix analysis*, Vol. 169 (Springer Science & Business Media, New York, 2013).
- [40] L. Banchi, N. Pancotti, and S. Bose, “Quantum gate learning in qubit networks: Toffoli gate without time-dependent control,” *npj Quantum Inf.* **2**, 16019 (2016).
- [41] L. Innocenti, L. Banchi, A. Ferraro, S. Bose, and M. Paternostro, “Supervised learning of time-independent hamiltonians for gate design,” preprint arXiv:1803.07119 (2018).
- [42] K. Mitarai, M. Negoro, M. Kitagawa, and K. Fujii, “Quantum circuit learning,” *Phys. Rev. A* **98**, 032309 (2018).
- [43] J. M. Arrazola, T. R. Bromley, J. Izaac, C. R. Myers, K. Brádler, and N. Killoran, “Machine learning method for state preparation and gate synthesis on photonic quantum computers,” *Quantum Sci. Technol.* **4**, 024004 (2019).
- [44] C. H. Bennett, G. Brassard, C. Crépeau, R. Jozsa, A. Peres, and W. K. Wootters, “Teleporting an unknown quantum state via dual classical and einstein-podolsky-rosen channels,” *Phys. Rev. Lett.* **70**, 1895 (1993).
- [45] S. Pirandola, J. Eisert, C. Weedbrook, A. Furusawa, and S. L. Braunstein, “Advances in quantum teleportation,” *Nat. Photon.* **9**, 641–652 (2015).
- [46] G. Bowen and S. Bose, “Teleportation as a depolarizing quantum channel, relative entropy, and classical capacity,” *Phys. Rev. Lett.* **87**, 267901 (2001).
- [47] T. P. W. Cope, L. Hetzel, L. Banchi, and S. Pirandola, “Simulation of non-pauli channels,” *Phys. Rev. A* **96**, 022323 (2017).
- [48] C. H. Bennett, D. P. DiVincenzo, J. A. Smolin, and W. K. Wootters, “Mixed-state entanglement and quantum error correction,” *Phys. Rev. A* **58**, 3824 (1996).
- [49] M. Christandl, F. Leditzky, C. Majenz, G. Smith, F. Speelman, and M. Walter, “Asymptotic performance of port-based teleportation,” preprint arXiv:1809.10751 (2018).
- [50] S. Lloyd, “Almost any quantum logic gate is universal,” *Phys. Rev. Lett.* **75**, 346 (1995).
- [51] N. Khaneja, T. Reiss, C. Kehlet, T. Schulte-Herbrüggen, and S. J. Glaser, “Optimal control of coupled spin dynamics: design of nmr pulse sequences by gradient ascent algorithms,” *J. Magn. Reson.* **172**, 296–305 (2005).
- [52] S. Boixo, S. V. Isakov, V. N. Smelyanskiy, R. Babbush, N. Ding, Z. Jiang, M. J. Bremner, J. M. Martinis, and H. Neven, “Characterizing quantum supremacy in near-term devices,” *Nat. Phys.* **14**, 595 (2018).
- [53] Seth Lloyd, Masoud Mohseni, and Patrick Rebentrost, “Quantum principal component analysis,” *Nat. Phys.* **10**, 631 (2014).
- [54] E. Stickel, “On the fréchet derivative of matrix functions,” *Linear Algebra and its Applications* **91**, 83–88 (1987).
- [55] S. N. Ravi, M. D. Collins, and V. Singh, “A deterministic nonsmooth frank wolfe algorithm with coresets guarantees,” preprint arXiv:1708.06714 (2017).
- [56] F. Yousefian, A. Nedić, and U. V. Shanbhag, “On stochastic gradient and subgradient methods with adaptive steplength sequences,” *Automatica* **48**, 56–67 (2012).
- [57] G. Lan, “The complexity of large-scale convex programming under a linear optimization oracle,” preprint arXiv:1309.5550 (2013).